The EMBO Journal (2013) 32, 2275–2286
www.embojournal.org

OPEN ACCESS TRANSPARENT PROCESS

THE EMBO JOURNAL

Neuronal carbonic anhydrase VII provides GABAergic excitatory drive to exacerbate febrile seizures

Eva Ruusuvuori[1,5], Antje K Huebner[2,5], Ilya Kirilkin[1,5], Alexey Y Yukin[1], Peter Blaesse[1,6], Mohamed Helmy[1], Hyo Jung Kang[3,7], Malek El Muayed[2,8], J Christopher Hennings[2], Juha Voipio[1], Nenad Šestan[3], Christian A Hübner[2] and Kai Kaila[1,4,*]

[1]Department of Biosciences, University of Helsinki, Helsinki, Finland, [2]Institute of Human Genetics, University Hospital Jena, Friedrich-Schiller-University Jena, Kollegiengasse 10, Jena, Germany, [3]Department of Neurobiology and Kavli Institute for Neuroscience, Yale University School of Medicine, New Haven, CT, USA and [4]Neuroscience Center, University of Helsinki, Helsinki, Finland

Brain carbonic anhydrases (CAs) are known to modulate neuronal signalling. Using a novel CA VII (*Car7*) knockout (KO) mouse as well as a CA II (*Car2*) KO and a CA II/VII double KO, we show that mature hippocampal pyramidal neurons are endowed with two cytosolic isoforms. CA VII is predominantly expressed by neurons starting around postnatal day 10 (P10). The ubiquitous isoform II is expressed in neurons at P20. Both isoforms enhance bicarbonate-driven GABAergic excitation during intense $GABA_A$-receptor activation. P13–14 CA VII KO mice show behavioural manifestations atypical of experimental febrile seizures (eFS) and a complete absence of electrographic seizures. A low dose of diazepam promotes eFS in P13–P14 rat pups, whereas seizures are blocked at higher concentrations that suppress breathing. Thus, the respiratory alkalosis-dependent eFS are exacerbated by GABAergic excitation. We found that CA VII mRNA is expressed in the human cerebral cortex before the age when febrile seizures (FS) occur in children. Our data indicate that CA VII is a key molecule in age-dependent neuronal pH regulation with consequent effects on generation of FS.

The EMBO Journal (2013) **32,** 2275–2286. doi:10.1038/emboj.2013.160; Published online 23 July 2013
Subject Categories: neuroscience
Keywords: carbonic anhydrase expression; chloride accumulation; $GABA_A$ receptor; human brain; hyperthermia

*Corresponding author. Department of Biosciences, University of Helsinki, POBox 65, FI-00014 Helsinki, Finland. Tel.: +358 9 19159860; E-mail: Kai.Kaila@Helsinki.Fi
[5]ER, AKH and IK contributed equally to this work.
[6]Present address: Institute of Physiology I, Westfälische Wilhelms-University Münster, D-48149 Münster, Germany
[7]Present address: Department of Life Science, Chung-Ang University, Seoul, Korea
[8]Present address: Division of Endocrinology, Metabolism and Molecular Medicine, Northwestern University Feinberg School of Medicine, Chicago, IL 60611, USA

Received: 9 January 2013; accepted: 20 June 2013; published online: 23 July 2013

Introduction

$GABA_A$-receptor ($GABA_AR$)-mediated signalling has a wide spectrum of functions in neurons and neuronal networks (Farrant and Kaila, 2007). Paradoxically, intense activation of GABAergic synapses in mature neurons may directly promote rather than suppress neuronal excitation (Alger and Nicoll, 1982; Kaila *et al*, 1997). We and others have previously demonstrated that, in the rat hippocampus, $GABA_AR$-mediated excitation is strictly dependent on the continuous replenishment of neuronal HCO_3^- by cytosolic carbonic anhydrase (CA) activity and suppressed by membrane-permeant inhibitors of CA (Staley *et al*, 1995; Kaila *et al*, 1997; Fujiwara-Tsukamoto *et al*, 2007; Viitanen *et al*, 2010). Whether HCO_3^--dependent GABAergic excitation has a role in the generation of seizures *in vivo* is not known.

CAs affect the kinetics and amplitudes of pH transients in distinct intra- and extracellular compartments (Chesler, 2003; Casey *et al*, 2010; Ruusuvuori and Kaila, 2013) and can thereby influence the function of a wide variety of proton-sensitive membrane proteins involved in neuronal signalling such as $GABA_ARs$ (Pasternack *et al*, 1996; Wilkins *et al*, 2005), *N*-methyl-D-aspartate receptors (Traynelis *et al*, 2010; Makani *et al*, 2012), acid-sensing ion channels (Waldmann *et al*, 1997), cation channels (Munsch and Pape, 1999; Williams *et al*, 2007; Enyedi and Czirjak, 2010) and gap junctions (Spray *et al*, 1981). In addition, pH transients can have modulatory actions on ion channels mediated by changes in fixed charges on the plasmalemmal surface (Velisek *et al*, 1994; Hille, 2001, see pp 653–654).

CA inhibitors such as acetazolamide and its more lipophilic derivatives have a long history as anticonvulsants, but the molecular targets and mechanisms of action at the neuronal network level are still poorly understood (Thiry *et al*, 2007; Supuran, 2008). The available inhibitors are not selective with respect to the 13 catalytically active isoforms that have been identified so far (Supuran, 2008) and may thus exert their actions within and outside the CNS. It is possible that their effects on neuronal functions are at least partly mediated by nitric oxide (Aamand *et al*, 2011) or calcium-activated potassium channels (Pickkers *et al*, 2001).

Using a novel CA VII knockout (KO) mouse as well as a CA II KO (Lewis *et al*, 1988) and a novel CA II/VII double KO, we show here that CA II and CA VII are the only cytosolic isoforms present in both somata and dendrites of mature hippocampal CA1 pyramidal neurons, with expression of CA VII commencing at postnatal day 10 (P10) and that of CA II at around P20. Immunoblots from glial or neuron/glial cultures showed that CA VII expression is restricted to neurons while CA II is present in both types of cells. After P30, the two isoforms are similarly effective in promoting GABAergic excitation.

In line with our previous data on rats (Schuchmann *et al*, 2006), hyperthermia generated a similar respiratory alkalosis in both wild-type (WT) and CA VII KO mice at P13–14. Typical experimental febrile seizures (eFS) with cortical electrographic seizure activity were observed in WT mice but not in the CA VII KOs. Diazepam potentiated excitatory GABAergic transmission *in vitro*, and a low concentration of the drug reduced the time to eFS onset in P14 rats *in vivo*. Consistent with a role in human febrile seizures (FS), we found that CA VII is present in the human cortex and hippocampus already at the perinatal stage, well before 6 months of age when FS are typically first observed (Berg and Shinnar, 1996; Stafstrom, 2002). Thus, CA VII is a key molecule in age-dependent neuronal pH regulation with consequent effects on generation of eFS.

Results

Generation of the CA VII KO mouse

We floxed exons 5–7 of the *Car7* gene (Figure 1A), and homologous recombination was verified by Southern blot analysis with a 3′ probe using an additional *Eco*RI site in the targeted allele. In two independent correctly targeted ES cell clones, we transiently expressed Cre-recombinase. The resulting subclones were screened for deletion of the DNA fragment flanked by the outer loxP sites. Two independent subclones were then injected into blastocysts and transferred to foster mice. The resulting chimeras were mated with C57BL/6 mice and produced offspring to heterozygous KO mice. Homozygous KO mice were born from heterozygous matings in the expected Mendelian ratio ($\sim$25%) and did not display any obvious phenotype within the age range used in the present experiments (up to P56, where P0 refers to the day of birth) or in the breeding animals used for about 1 year.

Expression patterns of CA VII mRNA and protein

Northern blot analysis in adult mouse tissues showed that CA VII is prominently expressed in the mature brain (Figure 1B). To detect CA VII at the protein level, a novel polyclonal antiserum against an epitope of murine CA VII was raised in rabbits and affinity-purified. In protein lysates of adult WT whole hippocampi, this antibody detected a band of an appropriate size of $\sim$30 kDa, which was absent from protein lysates prepared from the hippocampi of CA VII KO mice (Figure 1C). In WT mice, CA VII protein abundance increased in the hippocampus during postnatal maturation. Immunoblots on CA VII from lysates of glial and mixed neuron/glia cultures showed that, unlike CA II, CA VII is expressed in neurons but not in glia (Figure 1D). Using an antibody that is not validated in CA VII KO tissue, Bootorabi *et al* (2010) reported expression of CA VII in numerous mouse tissues including skeletal muscle and liver, while no signal was seen in the CNS. These data are in stark contrast with the mRNA expression analysis shown in Figure 1B and also with immunoblots based on our antibody in muscle and liver where no CA VII protein was detected (Supplementary Figure S1).

CA VII is the first functional cytosolic isoform expressed in somata of CA1 pyramidal neurons

Our previous results on rats showed a temporal coincidence between the developmental upregulation of CA VII mRNA and enhanced CA activity probed by CA inhibitors in pyramidal neurons (Ruusuvuori *et al*, 2004). Because the available cytosolic CA inhibitors are not isoform specific, these data do not exclude the possible presence of other neuronal CA isoforms. To overcome this problem, we examined the emergence of CA activity in somata of the hippocampal CA1 pyramidal neurons using BCECF fluorescence recording of intracellular pH (pH_i) in slices from neonatal, juvenile and adult WT and the three CA transgenic mice (CA VII KO, CA II KO and CA II/VII double KO) (Figure 2).

An abrupt developmental onset of cytosolic CA activity was detected in WT neurons at P10. The alkaline shifts measured in the somatic area upon CO_2/HCO_3^- withdrawal became faster and larger and the membrane-permeant CA inhibitor acetazolamide caused a clear suppression of the maximum rate of the alkalinization in 81% of P10–18 neurons ($n = 53$) (Figure 2A and B). In sharp contrast to WT, functional cytosolic CA was not detected in CA VII KO neurons at this age. The alkalinization was slow and insensitive to acetazolamide in all of the <P17 CA VII KO neurons ($n = 60$) and in 28 of 29 P17–18 CA VII KO neurons, similar to the pH_i response in WT neurons before the onset of CA expression ($n = 13$, WT neurons <P10) (Figure 2A and B). These results provide firm evidence for the conclusions that (i) the developmental upregulation of CA activity in the somatic area of mouse hippocampal CA1 pyramidal neurons at P10 is solely attributable to CA VII, and thus (ii) this is the *only cytosolic isoform* that shows catalytic activity in the P10–18 time window.

The expression of CA VII caused a small change in the baseline pH_i (Supplementary Figure S2), which can be readily explained by production of CO_2 within the slice (Voipio and Kaila, 1993).

Upregulation of cytosolic CA activity in somata of >P18 CA VII KO neurons is attributable to CA II

Surprisingly, an upregulation of CA activity was observed in neurons from CA VII KO mice at around P20 (Figure 2B and C). CA activity was observed in about 50% of >P18 neurons, and after P35 the percentage of CA VII KO cells showing catalytic activity was similar to that in WT.

Measurements of pH_i in CA II/VII double KO neurons demonstrated that they were completely devoid of cytosolic CA activity even after P35. In contrast to this, CA activity was detected in a roughly similar fraction in WT, CA VII KO and CA II KO neurons after P35 (83, 88 and 80%). After P25, the baseline of somatic pH_i was more acidotic compared with P14–15 neurons from WT and CA VII KO, and there was no longer a difference in the mean resting pH_i between the two genotypes (Supplementary Figure S2), implying that the presence of both CA VII and CA II, or of CA II alone, had an identical effect on baseline pH. Thus, experiments with the three KO transgenic mice show that the cytosol of mature CA1 pyramidal neuron somata in WT mice is endowed with two CA isoforms, CA II and CA VII.

Depolarizing dendritic GABA responses are promoted by CA II and CA VII

Next, we studied the developmental expression patterns of CA isoforms in the dendrites of pyramidal cells. To this end, we first used whole-cell recordings from CA1 pyramidal neurons in P12–16 WT and CA VII KO slices and examined GABAergic synaptic responses. Biphasic GABAergic

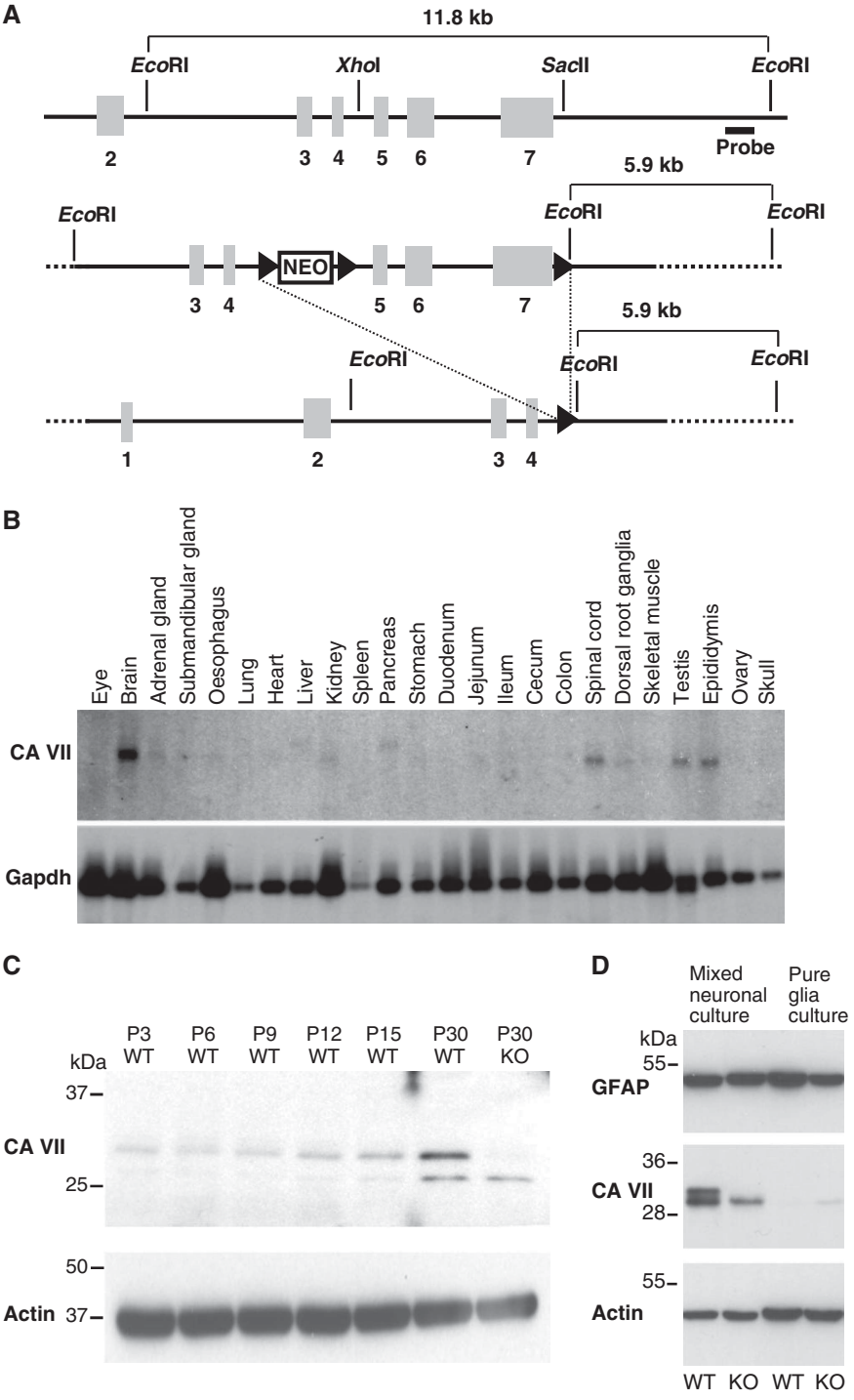

Figure 1 Generation of CA VII-deficient mice. (**A**) Targeting strategy for the *Car7* locus. Endogenous *Car7* locus (top). Targeting construct (middle). Targeted locus after Cre-mediated recombination (bottom). Exons are indicated as grey boxes and loxP sites as arrowheads. (**B**) Multiple tissue northern blot for CA VII. In the P56 mouse, CA VII is prominently expressed in the central nervous system including brain and spinal cord. *Gapdh* served as the loading control. (**C**) Developmental profile of CA VII protein expression. Western blot analysis of protein lysates of whole hippocampi shows increasing CA VII levels from P3 to P30. The band of the appropriate size (~30 kDa) was absent in protein lysates from KO tissue. (**D**) In western blots from protein lysates of cultured cells, CA VII was detected in mixed glia/neuron cultures but not in glia cell cultures. The presence of astrocytes in all cultures was confirmed by detection of GFAP. Actin served as the loading control in **C** and **D**.

responses were evoked with high-frequency stimulation applied at the border of *stratum radiatum (sr) and stratum lacunosum-moleculare (slm)* in the presence of ionotropic glutamate receptor and $GABA_BR$ antagonists. In both WT and CA VII KO neurons, this stimulation evoked a biphasic response consisting of an initial hyperpolarization followed by a prolonged depolarization, both of which were abolished by picrotoxin (Figure 3A). The gradual positive shift has been shown to closely reflect the HCO_3^--driven conductive net uptake of Cl^- (Viitanen *et al*, 2010). Importantly, the slope of the depolarizing shift measured under current clamp conditions was considerably slower in CA VII KO than in

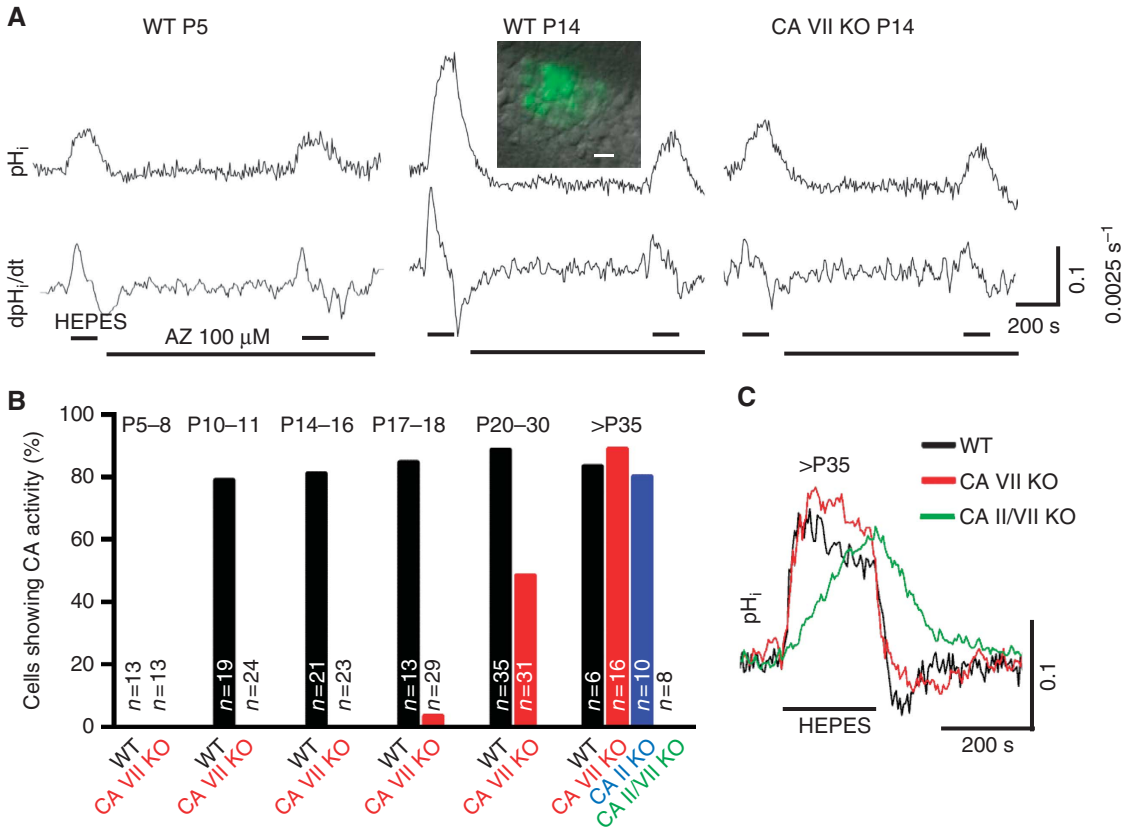

Figure 2 Development of cytosolic CA activity in mouse CA1 pyramidal neurons is based on sequential expression of isoforms VII and II. (**A**) Original single-cell pH_i traces and their time derivatives from P5 and P14 WT and P14 CA VII KO neurons (baseline pH_i 7.21, 7.13 and 7.11, respectively). Superfusion with CO_2/HCO_3^--free HEPES solution (upper horizontal bars) evoked an intracellular alkalinization, which in P14 WT was large and suppressed by 100 µM acetazolamide (AZ, lower horizontal bar), indicating the presence of CA activity (see Supplementary Materials and methods). The possible effect of AZ on extracellular CAs was excluded by adding 10 µM benzolamide (a poorly permeant CA inhibitor). Inset shows an overlay of the BCECF fluorescence signal and Dodt gradient contrast image of CA1 pyramidal neurons in P14 WT (scale bar 10 µm). (**B**) Summary of the results obtained using the cytosolic CA activity detection method shown in A and quantified as the percentage of cells showing cytosolic CA activity. Data from CA II KO and CA II/VII KO neurons were obtained only at >P35. The number of cells tested is indicated for each bar. The animal numbers for WT mice at the different age points was $n=3$ (P5–8), $n=2$ (P10–11), $n=3$ (P14–16), $n=2$ (P17–18), $n=2$ (P20–30) and $n=2$ (>P35); for CA VII KO mice the numbers were $n=3$ (P5–8), $n=2$ (P10–11), $n=5$ (P14–16), $n=3$ (P17–18), $n=4$ (P20–30) and $n=2$ (>P35); and for CA II KO and CA II/CA VII KO mice the number was $n=2$ (>P35). (**C**) Typical single pyramidal neuron pH_i responses evoked by withdrawal of CO_2/HCO_3^- (horizontal bar, HEPES) in slices from >P35 WT, CA VII KO and CA II/VII KO mice. The rate of rise and the amplitude of the alkaline shift are identical in WT (P39, baseline pH_i 7.01) and CA VII KO neurons (P40, 7.06), whereas alkalinization develops much more slowly in the CA II/VII KO (P46, 7.04).

WT neurons (Figure 3A). This indicates that the dendritic HCO_3^--dependent net uptake of Cl^- is strongly facilitated by CA activity in P12–P16 WT neurons. Measurements under voltage clamp conditions showed that the apparent charge transfer associated with single inhibitory post-synaptic currents was not different between the two genotypes (Supplementary Figure S3A).

In agreement with previous work on rat slices (Kaila *et al*, 1997; Ruusuvuori *et al*, 2004), the long-lasting GABAergic depolarization was able to induce action potential firing in WT neurons (Figure 3A). In striking contrast to this, action potentials were not observed in any of the 12 P12–16 CA VII KO neurons tested. A confounding factor in these experiments is a possible difference in the intrinsic excitability of WT versus CA VII KO neurons. We examined this by measuring the input resistance and the minimum current injection needed to trigger spiking (rheobase) in whole-cell mode, but no difference was found between neurons from WT and CA VII KO mice (Supplementary Figure S3B).

The role of the two cytosolic CA isoforms in the generation of dendritic depolarizing $GABA_A$ responses was examined using whole-cell recordings from CA1 pyramidal neurons in WT and CA VII KO slices at P12–16 (Figure 3B). Pressure microinjection of GABA at the border of *sr/slm* gave rise to biphasic membrane potential responses, where the depolarizing phase was much smaller in CA VII KOs than in WT. As expected, the depolarizing phase was selectively blocked in the absence of CO_2/HCO_3^- (in the HEPES buffered-solution).

That GABA is excitatory and induces neuronal firing in a CA VII-dependent manner in intact P12–16 WT neurons was clearly seen in field potential recordings (Figure 3C). In all slices from P12–16 WT animals, pressure injection of GABA at the border of *sr/slm* induced spiking and the number of spikes increased with the duration of the GABA puff (8 ms: 6.9 ± 2, 10 ms: 18.0 ± 3.8, 12 ms: 22.1 ± 4.7, 14 ms: 25.6 ± 6.0 and 16 ms: 29.3 ± 7.8). Spiking was fully blocked by the $GABA_A$-receptor antagonist SR 95531 (gabazine). In contrast, in slices from CA VII KO mice, GABA application evoked hardly any spiking even with the longest puff.

When examining intracellular GABA responses after P35 using GABA pressure injection as described above, no difference was observed between the WT, CA II KO and CA

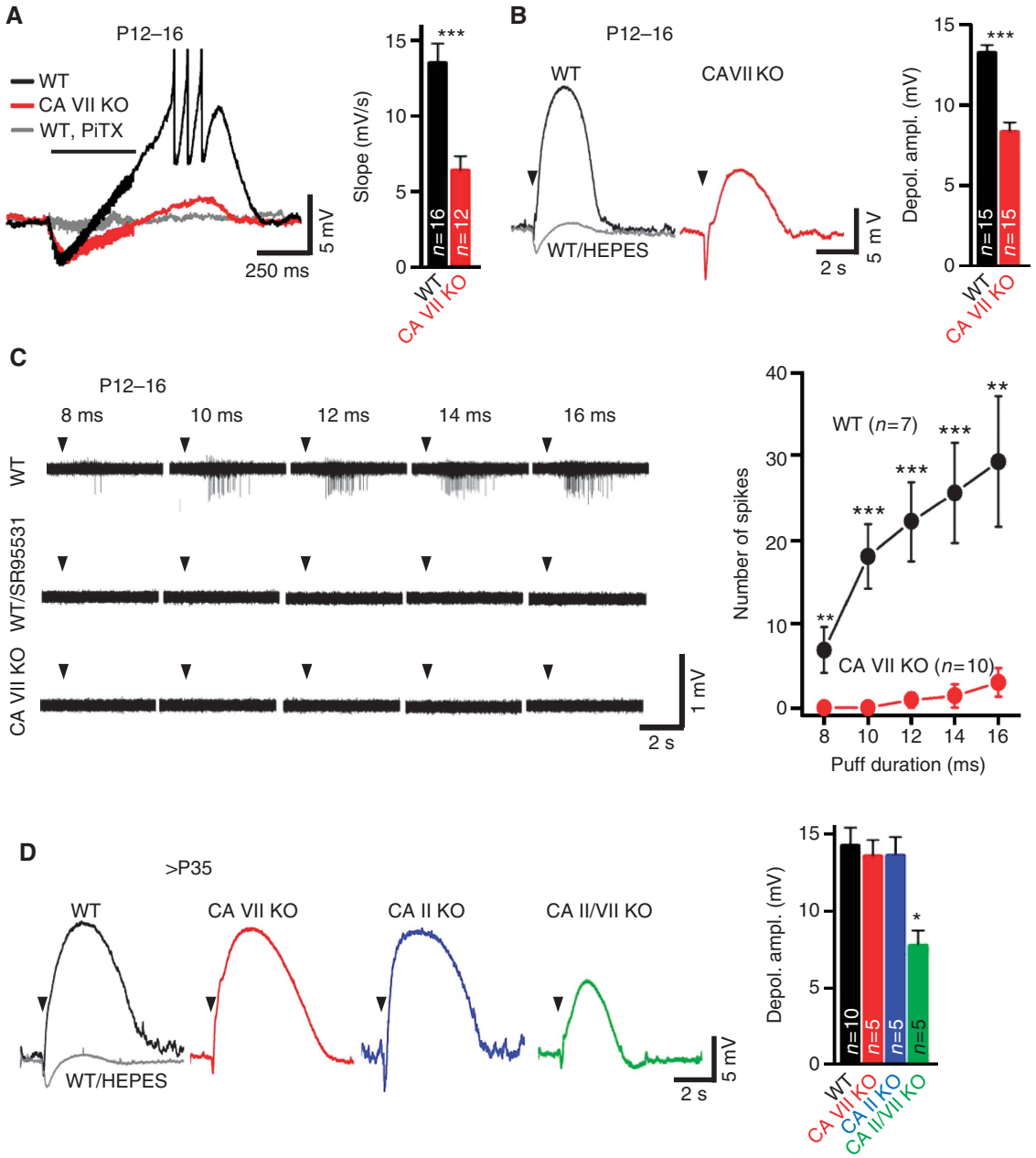

Figure 3 CA VII and CA II similarly enhance $GABA_A$R-mediated depolarization in CA1 pyramidal neurons. (**A**) Electrical stimulation (40 pulses, 100 Hz at *stratum radiatum/stratum lacunosum-moleculare* (*sr/slm)* border (horizontal bar)) in the presence of AP5/CNQX/CGP55845) evokes an excitatory GABAergic response in WT, but not in CA VII KO neurons. Picrotoxin blocked the biphasic response (PiTX 90 μM; $n = 3$/genotype). The mean initial slope of the depolarizing shift was faster in WT than in CA VII KO (13.53 ± 1.27 versus 6.39 ± 0.96 mV/s, $P < 0.001$, Student's *t*-test). The resting membrane potential of WT and CA VII KO neurons did not differ (− 71.0 ± 1.1 versus − 72.3 ± 1.4 mV, respectively; $n = 15$ neurons for both genotypes, $P = 0.47$, Student's *t*-test). (**B**) Microinjection of GABA (5 mM for 100 ms, *sr/slm* border in the presence of CGP55845/TTX, arrowheads) induced a pronounced depolarization in WT neurons (black) that was abolished in the absence of CO_2/HCO_3^- (grey). The depolarization was smaller in CA VII KO (red). Bar diagram illustrates GABAergic mean peak depolarization in P12–16 WT and CA VII KO (13.3 ± 0.5 versus 8.3 ± 0.6 mV, $P < 0.001$, Student's *t*-test). (**C**) In the presence of AP5/CNQX/CGP55845, microinjection of GABA (5 mM, *sr/slm* border) triggered SR 95531-sensitive field potential spikes in WT slices already upon 8-ms injection, while even 16-ms injection evoked hardly any spikes in CA VII KO (left). Mean number of spikes was plotted against GABA puff duration in P12–16 WT and CA VII KO ($P < 0.01$ and $P < 0.001$, Student's *t*-test; right). (**D**) After P35, depolarizations upon GABA microinjection (arrowheads) in the presence of CGP55845/TTX were indistinguishable in WT (black), CA VII KO (red) and CA II KO (blue) but smaller in CA II/VII KO (green). The depolarization in WT was abolished in the absence of CO_2/HCO_3^- (grey, $n = 5$). Bar diagram summarizes mean peak depolarization for each genotype (right; ANOVA, Bonferroni). $^*P < 0.05$, $^{**}P < 0.01$ and $^{***}P < 0.001$. Error bars denote s.e.m. and *n* is the number of slices (**C**) or cells tested (one cell per slice) (**A**, **B** and **D**).

VII KO neurons, indicating that both CA VII and CA II activity can promote depolarizing GABA responses in dendrites (Figure 3D, see also Kaila *et al*, 1997). In agreement with this, the dendritic GABA-evoked depolarization was much smaller in neurons from >P35 CA II/VII double KO animals (Figure 3D), and similar to that seen in P12–P16 CA VII KO neurons (Figure 3B). The presence of the attenuated but not fully abolished response in the double KO slices is consistent with the fact that, while replenishment of HCO_3^- by CA is rate-limiting for the GABAergic depolarization, the steady-

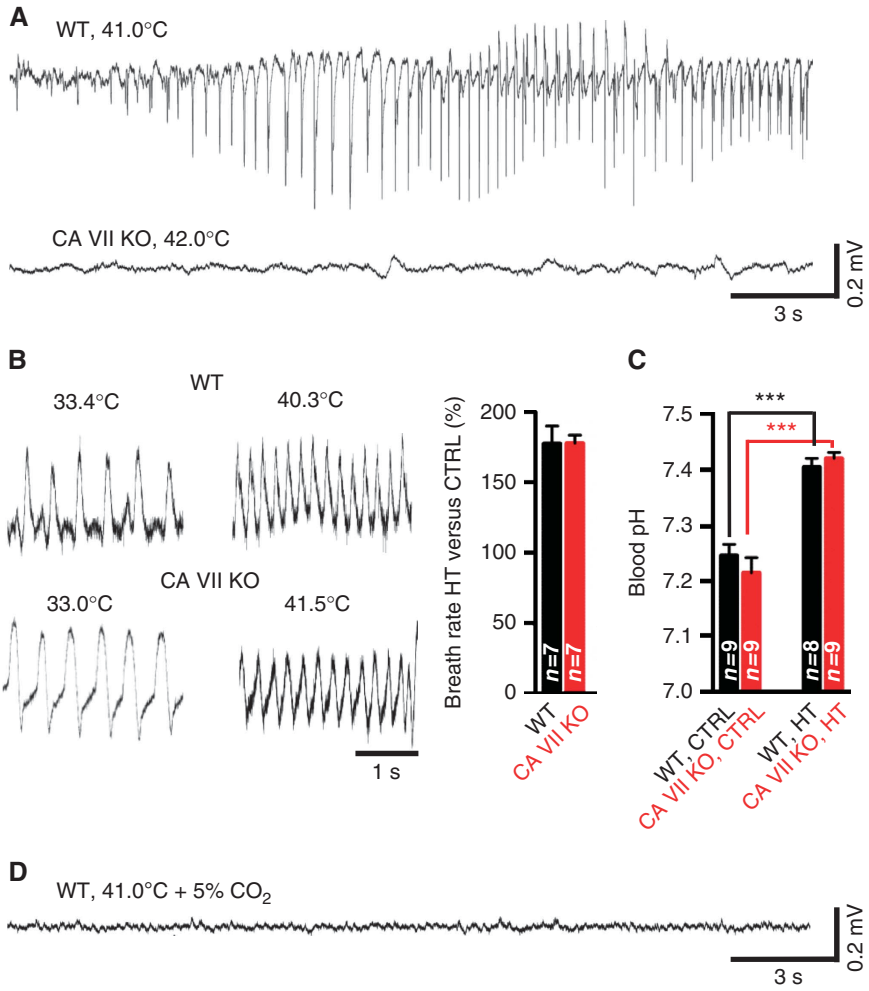

Figure 4 CA VII promotes experimental febrile seizures in P13–14 mice. (**A**) Representative raw traces of epidural EEG recordings during hyperthermia (HT) from a WT and a CA VII KO mouse. Seizures were reliably induced in WT ($n=9$) but not in CA VII KO ($n=7$). (**B**) Specimen recordings of breath rate from a WT and a CA VII KO mouse. The baseline breath rate (WT 153 ± 11 breaths/min and CA VII KO 157 ± 8 breaths/min) was increased during HT in both genotypes (WT 272 ± 28 breaths/min and CA VII KO 279 ± 12 breaths/min). The bar diagram summarizes the mean increase in breath rate in WT (177 ± 12%) and CA VII KO mice (178 ± 6%, $P=0.98$). (**C**) Hyperthermia caused a comparable alkalosis in blood pH in both WT and CA VII KO mice. The blood pH did not differ between the two genotypes under control conditions ($P=0.37$) or during HT ($P=0.44$). (**D**) Electrographic seizures were not detected in WT mice when hyperthermia was induced in the continuous presence of 5% CO_2 ($n=5$). Error bars denote s.e.m., all *P*-values are based on Student's *t*-test (***$P<0.001$), and animal number is given in bar diagrams. Rectal temperatures are given above the traces.

state HCO_3^- concentration of about 10 mM ($pH_i=6.9$, $pH_o=7.3$) is sufficient for a minor depolarizing action.

Lack of electrographic FS in CA VII KO mice

The seizure susceptibility of a large number of transgenic mice, including knock-in animals with gene variants that promote FS and related epileptiform syndromes in humans, has been tested using eFS triggered by exposure to hyperthermia (Meisler *et al*, 2001; Dube *et al*, 2005; van Gassen *et al*, 2008; Wimmer *et al*, 2010; Hill *et al*, 2011). The distinct developmental expression profiles of CA VII and II made it possible to specifically examine the role of isoform VII in the generation of eFS using P13–14 WT and CA VII KO mice. This developmental stage is considered relevant for comparisons with humans, in whom the peak incidence of FS is reached at the age of 18 months (Berg and Shinnar, 1996; Stafstrom, 2002). eFS were evoked using a pre-heated chamber as described before (Schuchmann *et al*, 2006).

As expected on the basis of previous work (Meisler *et al*, 2001; Dube *et al*, 2005; van Gassen *et al*, 2008), WT mice ($n=4$) when exposed to hyperthermia first showed normal explorative behaviour (score 0 in a behavioural scale of mouse eFS (van Gassen *et al*, 2008)) followed by hyperthermia-induced hyperactivity and escape responses (score 1). Thereafter, immobility and ataxia (score 2) were seen, after which seizures progressed to more severe manifestations including shaking, clonic seizures of one or more limbs (score 3), culminating in continuous tonic-clonic seizures (score 4) at a rectal temperature of 41.9 ± 1.1°C. Remarkably, none of the CA VII KO mice ($n=8$) showed progression of seizures beyond score 3 at similar temperature levels of 42.5 ± 0.5°C. Moreover, the seizure activity in the KO was atypical of eFS also in that it was interspersed with periods during which coordinated behaviour patterns such as walking and exploratory activity were seen, which never occurred in WT mice once seizures had progressed to the clonic stage.

Given the above qualitative difference in the behavioural hyperthermia effects between the WT and CA VII KO, we used EEG to gain more information on the underlying mechanisms.

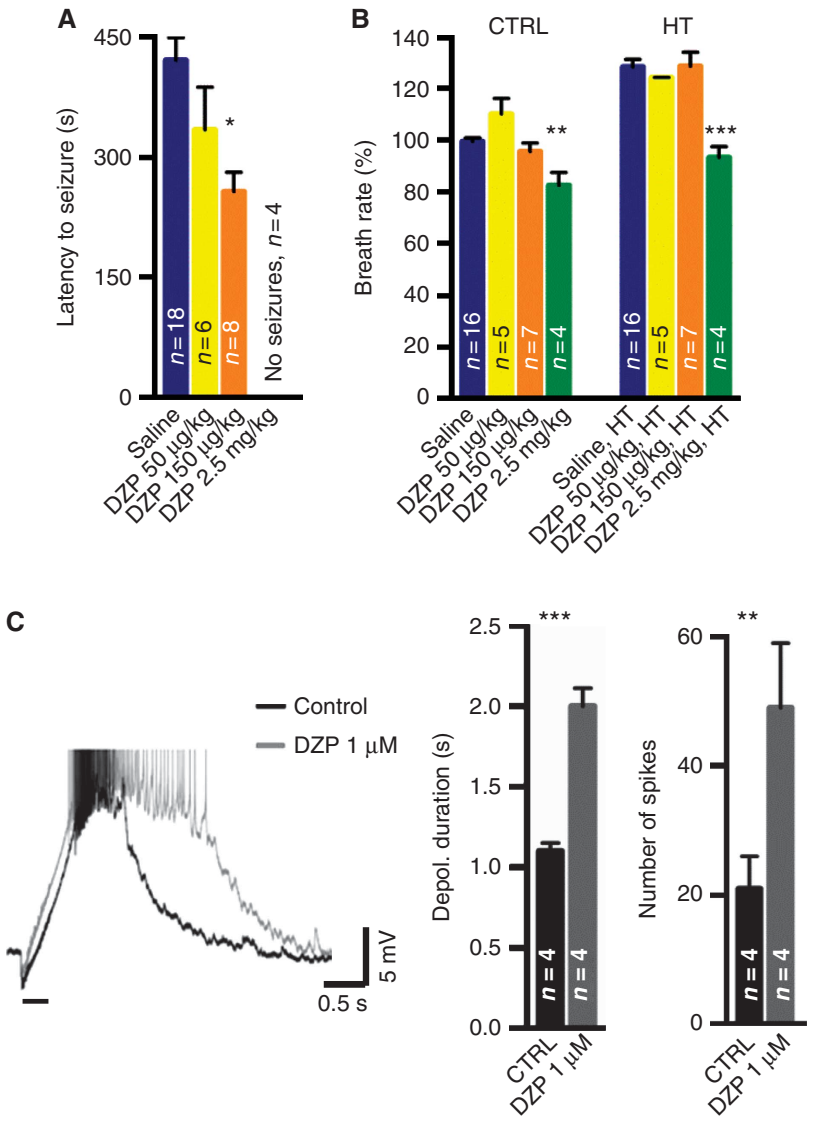

Figure 5 $GABA_A$-receptor-mediated modulation of experimental febrile seizures. (**A**) Diazepam (DZP, 150 µg/kg) reduced the latency to seizure onset in P14 rat pups ($P<0.05$). There was no statistical difference between 50 µg/kg and saline-injected animals. DZP 2.5 mg/kg completely blocked the seizures. DZP was given intraperitoneally 15 min before hyperthermia (HT) onset. (**B**) Diazepam given at 150 µg/kg did not affect the baseline breath rate, and HT induced an analogous increase in the breath rate in saline- and diazepam-injected rats ($P>0.05$). At a higher concentration (2.5 mg/kg), DZP suppressed breathing significantly ($P<0.01$) and HT caused only a small increase in the breath rate. (**C**) In slice preparation, DZP (1 µM) potentiated the high-frequency stimulation (40 pulses at 100 Hz, horizontal bar) -evoked $GABA_A$R-mediated depolarization. Sample trace from a slice from a P14 rat pup where stimulation to the border of *stratum radiatum* and *stratum lacunosum-moleculare* was given in the presence of AP5, CNQX and CGP 55845. The bar diagrams summarize the effects of DZP on the duration of the depolarization (time to half-maximum) and the number of action potentials associated with the depolarizing phase. *P*-values (*$P<0.05$, **$P<0.01$ and ***$P<0.001$) are based on ANOVA, Bonferroni (**A**, **B**) or Student's *t*-test (**C**), and error bars denote s.e.m. The number of animals (**A**, **B**) or cells (**C**) is indicated in bar diagrams.

Epidural EEG recordings showed that, in nine out of nine WT mice, electrographic seizures commenced within 24 ± 4 min after the onset of hyperthermia (Figure 4A). At this time point, the rectal temperature was 40.9 ± 0.4°C. The seizures were easily recognized as large-amplitude bursts of spikes (150–600 µV) with a frequency of about 2–4 Hz and duration of 10–60 s, which, notably, occurred mainly during periods of behavioural arrest as also reported by others (Dube *et al*, 2000). Because we have previously shown that a respiratory alkalosis is a major trigger of eFS (Schuchmann *et al*, 2006, 2011), we also measured the breath rates as well as blood pH values in the two genotypes. At the time of eFS onset in the WT, the breath rate had increased to 177 ± 12% (Figure 4B). In striking contrast to the WT, no electrographic seizures were observed in seven out of seven CA VII KO animals that were examined (Figure 4A). The rectal temperature (41.3 ± 0.4°C) and breath rate at 24 min after the onset of hyperthermia in CA VII KO animals were similar to those in WT animals (Figure 4B). Importantly, direct measurements of blood pH showed that hyperthermia induced a respiratory alkalosis with identical magnitude in both genotypes (Figure 4C). These data indicate that a suppression of systemic respiratory alkalosis does not explain the absence of eFS in the CA VII KO mice. Consistent with our earlier findings (Schuchmann *et al*, 2006), the generation of both behavioural and cortical electrographic eFS in WT mice were fully prevented when hyperthermia

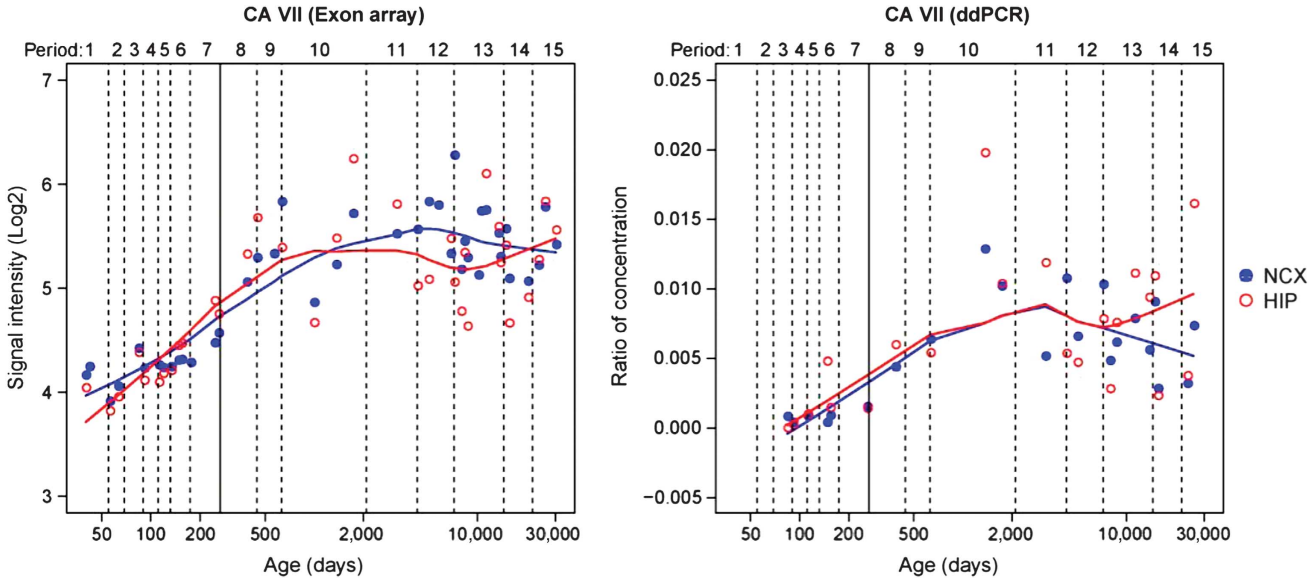

Figure 6 CA VII expression during human brain development. Line plots show the $\log_2$-transformed exon array signal intensity (left), and the normalized ratio of absolute copy number of CA VII to *Gapdh* by droplet digital PCR (ddPCR, right) in the neocortex (NCX) and hippocampus (HIP) from the early fetal period to late adulthood. The solid line between periods 7 and 8 separates the prenatal from the postnatal period.

was induced in the continuous presence of 5% CO_2 in air (Figure 4D). Finally, measurements of blood electrolytes showed no genotype-specific differences in control conditions or under hyperthermia (Supplementary Figure S4).

The above data raise the intriguing question whether CA VII-dependent GABAergic excitation contributes to the generation of cortical electrographic eFS. Hence, we performed behavioural experiments on P14 rat pups to examine whether enhancing $GABA_AR$ signalling by low doses of diazepam would facilitate the triggering of eFS. When diazepam was given at a very low dose (50 μg/kg intraperitoneally), latency to seizure onset decreased but the difference was not statistically significant from that seen in saline-injected animals (Figure 5A). However, a dose of 150 μg/kg resulted in a significant decrease in seizure latency. Importantly, neither of these two doses had a detectable effect on the baseline breath rate, and hyperthermia was associated with a similar increase in breath rate in rats injected with 50–150 μg/kg and in those injected with saline (Figure 5B). As could be expected (Hirtz and Nelson, 1983; Laorden *et al*, 1990), a higher dose of diazepam (2.5 mg/kg) prevented seizure generation in four of four rats tested, while the saline-injected control animals showed robust eFS (Figure 5A). At this concentration, diazepam suppressed the breath rate under control conditions and, under hyperthermia, only a modest increase in breathing was seen in the presence of the drug (Figure 5B).

In order to further examine the hypothesis that CA VII-dependent GABAergic excitation facilitates the generation of eFS, we evoked pharmacologically isolated excitatory GABAergic responses in P14 rat hippocampal slices. Consistent with the above hypothesis, the depolarizing phase as well as spiking evoked by the high-frequency stimulation was considerably enhanced by application of 1 μM diazepam (Figure 5C), with a maximum effect seen after 10 min of drug application.

As will be discussed below, the above *in vivo* and *in vitro* data as a whole suggest that eFS are facilitated by GABAergic excitation and that a low concentration of diazepam potentiates these effects by a selective action on $GABA_ARs$ (Eghbali *et al*, 1997). The suppression of eFS by a high dose of diazepam is readily explained by the suppression of breathing (Figure 5B).

Spatiotemporal expression patterns of human CA VII in the developing brain

We used exon array analysis and droplet digital PCR to examine the developmental expression of CA VII in the human neocortex and hippocampus (see Supplementary Materials and methods). Our previous study on the human brain transcriptome identified 29 modules corresponding to specific spatiotemporal expression patterns by weighted gene co-expression network analysis (Kang *et al*, 2011). Here, it is of much interest that, among them, CA VII was classified as a member of M2 (Supplementary Figure S5), a main module including 2745 genes, which is interpreted as a module related to synaptic transmission based on functional annotations using gene ontology (Kang *et al*, 2011). Our present data show that CA VII expression is markedly increased in the human neocortex and hippocampus during the perinatal period and sustained until late adulthood (Figure 6). Thus, an association between CA VII and epileptiform syndromes is not excluded at any stage of human neocortical and hippocampal development.

Discussion

Distinct CA isoforms exert a profound modulatory influence on the functions of a wide variety of voltage-gated channels, excitatory and inhibitory synapses and gap junctions (see Introduction). Because isoform-specific CA inhibitors are not available, we used gene disruption of two cytosolic isoforms, CA II and CA VII, separately and in combination to demonstrate the following: (i) CA activity is fully attributable to these two isoforms in the somata and dendrites of mature mouse CA1 pyramidal neurons; (ii) the two isoforms are sequentially expressed in the developing hippocampus, with expression of CA VII commencing at P10 and that of CA II at

around P20; (iii) in contrast to CA II, CA VII is not expressed in glia; (iv) both isoforms are able to promote HCO_3^--dependent GABAergic depolarization and excitation triggered by intense $GABA_A$R activation in mature neurons. This kind of information is crucial for understanding the mechanisms of pH-dependent modulation of neuronal and neuronal network functions in the developing and mature brain (Kaila and Ransom, 1998; Schuchmann *et al*, 2009; Casey *et al*, 2010; Tolner *et al*, 2011; Magnotta *et al*, 2012). We also show here that (v) excitatory CA VII-dependent GABA signalling promotes eFS at P14, and the relevance of this finding is underscored by the observation (vi) that CA VII is expressed in the human cortex perinatally, well in advance of the age of 6 months when FS are first seen in children (Berg and Shinnar, 1996; Stafstrom, 2002).

Our previous work on rat hippocampal slices has demonstrated that the emergence of excitatory HCO_3^--dependent $GABA_A$R-mediated responses in CA1 neurons (Kaila *et al*, 1997) coincides with the onset of CA VII mRNA expression at around P10–12 (Ruusuvuori *et al*, 2004). However, these data demonstrate a correlation but not a cause–effect link between CA VII expression and GABAergic excitation because the possibility remained that some other, unidentified isoform might have been expressed in parallel with CA VII. The present data, which are based on the use of a novel CA VII KO mouse as well as a CA II KO (Lewis *et al*, 1988) and a CA II/CA VII double KO, clearly indicate that the two isoforms are sequentially expressed. CA VII is the only cytosolic CA isoform during P10–P18, while the two isoforms are co-expressed starting at around P20. Given the steeply increasing interest in the physiology, pathophysiology and pharmacology of individual CA isoforms (Supuran, 2008), this kind of information is of immense value in the design and evaluation of experiments on neuronal CAs, and makes the hippocampal developmental time window of ~P12–16 (see Figure 2) eminently suited for examining the properties of CA VII in isolation. This isoform is interesting in that it is mainly expressed in the brain; moreover, in brain parenchyma its expression is restricted to neurons. The ubiquitous CA II isoform is expressed in both neurons and glia and abundantly outside the CNS (Ghandour *et al*, 1980; Wang *et al*, 2002; Supuran, 2008). Notably, the complete absence of CA activity in pyramidal neurons before P10 and in CA II/CA VII double KO neurons at all ages clearly shows that mature pyramidal neurons express only these two cytosolic isoforms.

Somatodendritic developmental expression of CA II and CA VII in pyramidal neurons

As demonstrated by the present somatic pH_i recordings and excitatory dendritic $GABA_A$R responses, the subcellular somatodendritic expression patterns of CA VII and CA II do not differ from each other. Moreover, both isoforms were equally effective in promoting somatic CO_2-dependent pH shifts separately from, and in combination with, each other. The intrinsic catalytic rates of CA II and CA VII are extremely high (Earnhardt *et al*, 1998), and hence it is obvious that the present assay (see Figure 2) does not reflect the kinetic properties of these two isoforms. Nevertheless, our data strongly suggest that neither isoform acting in isolation would be rate-limiting for pH_i changes during major physiological and pathophysiological acid-base shifts.

A possible explanation for the presence of two cytosolic CA isoforms after P20 is that they show differences in their biochemical functions other than (de)hydration of CO_2, such as esterase/phosphatase activity (Innocenti *et al*, 2008). Furthermore, the HCO_3^- transporters make a significant contribution to neuronal pH regulation (Hentschke *et al*, 2006; Jacobs *et al*, 2008; Sinning *et al*, 2011). By forming isoform-specific metabolons with distinct acid-base transporters, CA II and VII may contribute to developmentally and spatially distinct pH_i microdomains (Sterling *et al*, 2001; Becker and Deitmer, 2007; see also Boron, 2010; Stridh *et al*, 2012). Moreover, recent work suggests that CA VII acts as scavenger of oxygen radicals (Truppo *et al*, 2012), which fits well with the large increase in cortical ocidateve energy metabolism taking place at the time of onset of CA VII expression (Erecinska *et al*, 2004).

GABAergic excitation is promoted by both CA VII and CA II

Work on single crayfish muscle fibres and neurons originally demonstrated that the net efflux of intracellular HCO_3^- across $GABA_A$Rs leads to GABAergic depolarization by exerting a direct depolarizing action and, indirectly, by facilitating conductive uptake of Cl^- (Kaila and Voipio, 1987; Kaila *et al*, 1989; Voipio *et al*, 1991). The $GABA_A$R-mediated CA-dependent acidosis is readily explained by the fact that HCO_3^- is a substrate of cytosolic CAs, and a conductive net loss of HCO_3^- will by necessity shift the balance of the CA-catalysed (de)hydration reaction to more acidic pH_i values (Kaila *et al*, 1990; Luckermann *et al*, 1997). Accordingly, in mammalian neurons and especially in their dendrites, which have a much larger surface-to-volume ratio (Qian and Sejnowski, 1990), CA activity is generally thought to be necessary for maintaining the supply of intracellular HCO_3^- that drives GABAergic depolarizing and excitatory responses (Pasternack *et al*, 1993; Viitanen *et al*, 2010). In the present work, we addressed the roles of the two isoforms in the generation of HCO_3^--dependent GABAergic depolarization. Our data show that CA VII has a unique role in promoting Cl^- accumulation (Viitanen *et al*, 2010) and consequent depolarizing GABAergic responses during P10–18, a time window that is known to be associated with a heightened proneness to epileptogenesis in rodents (Swann *et al*, 1993; Gloveli *et al*, 1995). The co-expression of isoforms VII and II starting at P20 had no obvious effect on the $GABA_A$R-mediated depolarization.

Role of CA VII-dependent excitatory GABA transmission in the generation of eFS

The molecular and neuronal network mechanisms underlying eFS have been extensively studied in various inbred and mutant mouse strains at the age of P14 (van Gassen *et al*, 2008; Wimmer *et al*, 2010). This is a very intriguing time point in the present context, because it enables a comparison of susceptibility to eFS of mice that have, or are completely devoid of, cytosolic CA in pyramidal neurons—that is, the WT and CA VII KO mice, respectively.

We have previously shown that a respiratory alkalosis promotes the generation of eFS in rodents (Schuchmann *et al*, 2006), and a recent retrospective clinical study has shown that a respiratory alkalosis is characteristic of FS in children (Schuchmann *et al*, 2011). Notably, the present data on breath rates and direct measurements of blood pH show

that CA VII plays no role in hyperthermia-induced respiratory alkalosis in rodents. Here, one should recall that the non-catalysed (de)hydration of CO_2 has a half-time of 8 s (Geers and Gros, 2000) at a typical physiological temperature. CA activity is therefore not likely to be important for the extracellular and consequent intracellular pH changes (*cf.* Ruusuvuori *et al*, 2010) that are associated with the slow hyperthermia-induced respiratory alkalosis, which has a time-to-seizure induction of about 20 min. In contrast, intraneuronal CA activity is needed for the fast replenishment of HCO_3^- and consequent net uptake of Cl^-, which are key mechanisms in the generation of excitatory HCO_3^--dependent GABAergic responses (Ruusuvuori *et al*, 2004; Viitanen *et al*, 2010). Indeed, the present EEG data indicate that CA VII plays a central role in the generation of electrographic seizure activity associated with eFS in the cortex of P14 mice. The hypothesis that CA VII facilitates eFS by boosting GABAergic excitation is supported by two lines of evidence: (i) the behavioural eFS in P14 rats were enhanced by a low dose of diazepam, which is likely to act solely on $GABA_A$Rs (Eghbali *et al*, 1997), while a high concentration blocked seizures; and (ii) parallel *in vitro* experiments showed that the excitatory GABAergic response was markedly potentiated by 1 μM diazepam. Interestingly, a recent paper has demonstrated an enhancement of GABAergic transmission in the $GABRG2^{R43/Q43}$ knock-in mouse model of human FS (Hill *et al*, 2011).

The above data point to a facilitatory role for CA VII activity and consequent GABAergic excitation in the generation of FS. Importantly, the difference between genotypes in eFS susceptibility cannot be attributed to a difference in body temperature at the onset of the seizures. The dual effects of diazepam *in vivo* raise the intriguing possibility (see also Schuchmann *et al*, 2011) that the high therapeutic concentrations needed for suppression of FS in children exert their action via suppression of breathing rather than acting directly on the neuronal networks that are immediately responsible for the generation of FS. Indeed, it is a well-known fact that high concentrations of diazepines interfere with respiratory functions, especially in children (Orr *et al*, 1991; Tasker, 1998; Norris *et al*, 1999; Appleton *et al*, 2008). The expected outcome is block of the respiratory alkalosis with consequent suppression of FS.

Importantly, the expression of CA VII in the human cortex and hippocampus, as demonstrated in the exon array and droplet digital PCR analyses, already starts perinatally, while FS are typically seen in children at 6 months of age with the incidence peaking at 1.5 years (Berg and Shinnar, 1996; Stafstrom, 2002). CA inhibitors have been used for decades as anticonvulsant agents, but their side effects, including interference with bone formation (Lehenkari *et al*, 1998), preclude their long-term use in children. Notably, CA VII shows an expression profile that is mainly neuronal. Thus, designing isoform-specific inhibitors of CA VII has much potential as a novel approach in the treatment of FS and possibly of other epileptiform syndromes.

Materials and methods

Animal experiments were approved by the responsible local institutions and complied with the regulations of the US National Institutes of Health and with those of the Society for Neuroscience (USA). Researchers were blind to the genotype during experiments and data analysis. Human tissues were collected as before (Kang *et al*, 2011) after obtaining parental or next-of-kin consent and with approval by the relevant institutional review boards.

Generation of CA VII KO mice

The *Car7* gene was disrupted by homologous recombination in ES cells and blastocyst injection as detailed in Results and in Supplementary Materials and methods.

Northern analysis

Northern blot analysis was performed with RNA isolated from various tissues of adult mouse as described previously (Jacobs *et al*, 2008). The probe corresponded to nucleotides 210–492 of the *Car7* reference sequence (NM_053070.3). *Gapdh* served as a loading control.

Antibody generation and western analysis

The CA VII antiserum was raised in rabbits against the epitope DNFRPPQPLKGRVVK (amino acids 245–259) of the CA VII protein (accession number NM_053070.3) coupled via an N-terminal cysteine to keyhole limpet haemocyanin and affinity-purified. For western blots shown in Figure 1, 10 μg protein lysates from whole hippocampi or from cultured cells was separated on reducing 12% SDS–polyacrylamide gels and blotted on to a PVDF membrane as described in Sinning *et al*, 2011. Blots were probed with the rabbit CA VII antibody at a dilution of 1:250. Detection was performed with the chemiluminescence ECL Kit (Amersham Biosciences). Comparison of immunostainings for CA VII on brain sections from WT and KO mice revealed that our antibody was not suitable for immunolocalization studies because of unspecific staining. Mixed neuron/glia cultures or glial cell cultures were performed as described previously (Boettger *et al*, 2003). For additional western blots, see Supplementary Materials and methods.

Generation of CA II/VII double KO mice

Animals heterozygous for both CA II and CA VII alleles were used to generate CA II/VII double KO mice. For more details on the CA II/VII double KO and genotyping, see Supplementary Materials and methods.

Electrophysiology and pH_i fluorescence imaging

For details on electrophysiological recordings and BCECF fluorescence imaging of pH_i from hippocampal CA1 pyramidal neurons, see Supplementary Materials and methods.

EEG recordings and eFS induction

In P14 rat pups, eFS were induced using a pre-heated chamber as described elsewhere (Schuchmann *et al*, 2006). For intracranial EEG recordings and for detection of behavioural hyperthermia effects in P13–14 mice, the temperature of the chamber was set to 43 ± 1°C. For details see Supplementary Materials and methods.

Blood analysis

GEM 4000 (Instrumentation Laboratory, Bedford, MA) was used in the analysis of trunk blood electrolytes and pH. Arteriovenous blood (80 μl) from control mice and from mice that underwent hyperthermia was collected after decapitation.

CA VII detection in developing human brain

Exon array analysis was performed as previously described (Kang *et al*, 2011). For secondary validation using droplet digital PCR analysis, an aliquot of the total RNA that was previously extracted from each brain region was used. For more details, see Supplementary Materials and methods.

Statistical analysis

All numerical data are expressed as mean ± s.e.m. Statistical analyses of data were performed with two-tailed Student's *t*-test or with ANOVA, Bonferroni as appropriate. *P*-values are given in the figure legends.

Supplementary data

Supplementary data are available at *The EMBO Journal* Online (http://www.embojournal.org).

Acknowledgements

This study was supported by grants from the Academy of Finland, the Sigrid Jusélius Foundation, and the Jane and Aatos Erkko Foundation to KK, by grants from the DFG to CAH and by grant from NIMH (MH081896) to NS. KK is a member of the Finnish Center of Excellence in Molecular and Integrative Neuroscience Research.

Author contributions: ER, AKH, IK, HJK, JV, NS, CAH and KK designed the research; AKH, IK, PB, MH, AYY, HJK, MEM and JCH performed the research; ER, AKH, IK, PB, MH, AYY, HJK, MEM, JCH, JV, NS, CAH and KK analysed the data; and ER, IK, HJK, JV, NS, CAH and KK wrote the paper.

Conflict of interest

The authors declare that they have no conflict of interest.

References

Aamand R, Skewes J, Moller A, Fago A, Roepstorff A (2011) Enhancing effects of acetazolamide on neuronal activity correlate with enhanced visual processing ability in humans. *Neuropharmacology* **61:** 900–908

Alger BE, Nicoll RA (1982) Pharmacological evidence for two kinds of GABA receptor on rat hippocampal pyramidal cells studied *in vitro*. *J Physiol* **328:** 125–141

Appleton R, Macleod S, Martland T (2008) Drug management for acute tonic-clonic convulsions including convulsive status epilepticus in children. *Cochrane Database Syst Rev*: CD001905

Becker HM, Deitmer JW (2007) Carbonic anhydrase II increases the activity of the human electrogenic Na^+/HCO_3^- cotransporter. *J Biol Chem* **282:** 13508–13521

Berg AT, Shinnar S (1996) Complex febrile seizures. *Epilepsia* **37:** 126–133

Boettger T, Rust MB, Maier H, Seidenbecher T, Schweizer M, Keating DJ, Faulhaber J, Ehmke H, Pfeffer C, Scheel O, Lemcke B, Horst J, Leuwer R, Pape HC, Volkl H, Hübner CA, Jentsch TJ (2003) Loss of K-Cl co-transporter KCC3 causes deafness, neurodegeneration and reduced seizure threshold. *EMBO J* **22:** 5422–5434

Bootorabi F, Janis J, Smith E, Waheed A, Kukkurainen S, Hytonen V, Valjakka J, Supuran CT, Vullo D, Sly WS, Parkkila S (2010) Analysis of a shortened form of human carbonic anhydrase VII expressed *in vitro* compared to the full-length enzyme. *Biochimie* **92:** 1072–1080

Boron WF (2010) Evaluating the role of carbonic anhydrases in the transport of HCO3–related species. *Biochim Biophys Acta* **1804:** 410–421

Casey JR, Grinstein S, Orlowski J (2010) Sensors and regulators of intracellular pH. *Nat Rev Mol Cell Biol* **11:** 50–61

Chesler M (2003) Regulation and modulation of pH in the brain. *Physiol Rev* **83:** 1183–1221

Dube C, Chen K, Eghbal-Ahmadi M, Brunson K, Soltesz I, Baram TZ (2000) Prolonged febrile seizures in the immature rat model enhance hippocampal excitability long term. *Ann Neurol* **47:** 336–344

Dube C, Vezzani A, Behrens M, Bartfai T, Baram TZ (2005) Interleukin-1beta contributes to the generation of experimental febrile seizures. *Ann Neurol* **57:** 152–155

Earnhardt JN, Qian MZ, Tu CK, Lakkis MM, Bergenhem NCH, Laipis PJ, Tashian RE, Silverman DN (1998) The catalytic properties of murine carbonic anhydrase VII. *Biochemistry* **37:** 10837–10845

Eghbali M, Curmi JP, Birnir B, Gage PW (1997) Hippocampal GABA(A) channel conductance increased by diazepam. *Nature* **388:** 71–75

Enyedi P, Czirjak G (2010) Molecular background of leak K^+ currents: Two-pore domain potassium channels. *Physiol Rev* **90:** 559–605

Erecinska M, Cherian S, Silver IA (2004) Energy metabolism in mammalian brain during development. *Prog Neurobiol* **73:** 397–445

Farrant M, Kaila K (2007) The cellular, molecular and ionic basis of GABAA receptor signalling. *Prog Brain Res* **160:** 59–87

Fujiwara-Tsukamoto Y, Isomura Y, Imanishi M, Fukai T, Takada M (2007) Distinct types of ionic modulation of GABA actions in pyramidal cells and interneurons during electrical induction of hippocampal seizure-like network activity. *Eur J Neurosci* **25:** 2713–2725

Geers C, Gros G (2000) Carbon dioxide transport and carbonic anhydrase in blood and muscle. *Physiol Rev* **80:** 681–715

Ghandour MS, Langley OK, Vincendon G, Gombos G, Filippi D, Limozin N, Dalmasso C, Laurent G (1980) Immunochemical and immunohistochemical study of carbonic anhydrase-II in adult rat cerebellum—a marker for oligodendrocytes. *Neuroscience* **5:** 559–571

Gloveli T, Albrecht D, Heinemann U (1995) Properties of low Mg^{2+} induced epileptiform activity in rat hippocampal and entorhinal cortex slices during adolescence. *Dev Brain Res* **87:** 145–152

Hentschke M, Wiemann M, Hentschke S, Kurth I, Hermans-Borgmeyer I, Seidenbecher T, Jentsch TJ, Gal A, Hübner CA (2006) Mice with a targeted disruption of the Cl^-/HCO_3^- exchanger AE3 display a reduced seizure threshold. *Mol Cell Biol* **26:** 182–191

Hill EL, Hosie S, Mulligan RS, Richards KL, Davies PJ, Dube CM, Baram TZ, Reid CA, Jones MV, Petrou S (2011) Temperature elevation increases GABA(A)-mediated cortical inhibition in a mouse model of genetic epilepsy. *Epilepsia* **52:** 179–184

Hille B (2001) *Ionic channels of excitable membranes*. Third Edition. Sunderland, Massachusetts: Sinauer Associates

Hirtz DG, Nelson KB (1983) The natural history of febrile seizures. *Annu Rev Med* **34:** 453–471

Innocenti A, Scozzafava A, Parkkila S, Puccetti L, De Simone G, Supuran CT (2008) Investigations of the esterase, phosphatase, and sulfatase activities of the cytosolic mammalian carbonic anhydrase isoforms I, II, and XIII with 4-nitrophenyl esters as substrates. *Bioorg Med Chem Lett* **18:** 2267–2271

Jacobs S, Ruusuvuori E, Sipila ST, Haapanen A, Damkier HH, Kurth I, Hentschke M, Schweizer M, Rudhard Y, Laatikainen LM, Tyynela J, Praetorius J, Voipio J, Hubner CA (2008) Mice with targeted Slc4a10 gene disruption have small brain ventricles and show reduced neuronal excitability. *Proc Natl Acad Sci USA* **105:** 311–316

Kaila K, Lamsa K, Smirnov S, Taira T, Voipio J (1997) Long-lasting GABA-mediated depolarization evoked by high- frequency stimulation in pyramidal neurons of rat hippocampal slice is attributable to a network-driven, bicarbonate-dependent K^+ transient. *J Neurosci* **17:** 7662–7672

Kaila K, Pasternack M, Saarikoski J, Voipio J (1989) Influence of GABA-gated bicarbonate conductance on potential, current and intracellular chloride in crayfish muscle fibres. *J Physiol* **416:** 161–181

Kaila K, Ransom BR (1998) *pH and Brain Function*. New York: Wiley-Liss, Inc.

Kaila K, Saarikoski J, Voipio J (1990) Mechanism of action of GABA on intracellular pH and on surface pH in crayfish muscle fibres. *J Physiol* **427:** 241–260

Kaila K, Voipio J (1987) Postsynaptic fall in intracellular pH induced by GABA-activated bicarbonate conductance. *Nature* **330:** 163–165

Kang HJ *et al* (2011) Spatio-temporal transcriptome of the human brain. *Nature* **478:** 483–489

Laorden ML, Carrillo E, Miralles FS, Puig MM (1990) Effects of diltiazem on hyperthermia induced seizures in the rat pup. *Gen Pharmacol* **21:** 313–315

Lehenkari P, Hentunen TA, Laitala-Leinonen T, Tuukkanen J, Vaananen HK (1998) Carbonic anhydrase II plays a major role in osteoclast differentiation and bone resorption by effecting the steady state intracellular pH and Ca^{2+}. *Exp Cell Res* **242:** 128–137

Lewis SE, Erickson RP, Barnett LB, Venta PJ, Tashian RE (1988) N-ethyl-N-nitrosurea induced mutation at the mouse Car-2 locus - an animal model for human carbonic anhydrase II-deficiency syndrome. *Proc Natl Acad Sci USA* **85:** 1962–1966

Luckermann M, Trapp S, Ballanyi K (1997) GABA- and glycine-mediated fall of intracellular pH in rat medullary neurons *in situ*. *J Neurophysiol* **77:** 1844–1852

Magnotta VA, Heo HY, Dlouhy BJ, Dahdaleh NS, Follmer RL, Thedens DR, Welsh MJ, Wemmie JA (2012) Detecting activity-evoked pH changes in human brain. *Proc Natl Acad Sci USA* **109:** 8270–8273

Makani S, Chen HY, Esquenazi S, Shah GN, Waheed A, Sly WS, Chesler M (2012) NMDA receptor-dependent afterdepolarizations are curtailed by carbonic anhydrase 14: regulation of a short-term postsynaptic potentiation. *J Neurosci* **32:** 16754–16762

Meisler MH, Kearney J, Ottman R, Escayg A (2001) Identification of epilepsy genes in human and mouse. *Annu Rev Genet* **35:** 567–588

Munsch T, Pape HC (1999) Modulation of the hyperpolarization-activated cation current of rat thalamic relay neurones by intracellular pH. *J Physiol* **519**(Pt 2): 493–504

Norris E, Marzouk O, Nunn A, McIntyre J, Choonara I (1999) Respiratory depression in children receiving diazepam for acute seizures: a prospective study. *Dev Med Child Neurol* **41:** 340–343

Orr RA, Dimand RJ, Venkataraman ST, Karr VA, Kennedy KJ (1991) Diazepam and intubation in emergency treatment of seizures in children. *Ann Emerg Med* **20:** 1009–1013

Pasternack M, Smirnov S, Kaila K (1996) Proton modulation of functionally distinct $GABA_A$ receptors in acutely isolated pyramidal neurons of rat hippocampus. *Neuropharmacology* **35:** 1279–1288

Pasternack M, Voipio J, Kaila K (1993) Intracellular carbonic anhydrase activity and its role in GABA-induced acidosis in isolated rat hippocampal pyramidal neurones. *Acta Physiol Scand* **148:** 229–231

Pickkers P, Hughes AD, Russel FG, Thien T, Smits P (2001) *In vivo* evidence for K(Ca) channel opening properties of acetazolamide in the human vasculature. *Br J Pharmacol* **132:** 443–450

Qian N, Sejnowski TJ (1990) When is an inhibitory synapse effective? *Proc Natl Acad Sci USA* **87:** 8145–8149

Ruusuvuori E, Kaila K (2013) Carbonic anhydrases and brain pH in the control of neuronal excitability. In *Carbonic Anhydrase: Mechanism, Regulation, Links to Disease, and Industrial Applications*, Frost SC, McKenna R (eds), Springer (in press)

Ruusuvuori E, Kirilkin I, Pandya N, Kaila K (2010) Spontaneous network events driven by depolarizing GABA action in neonatal hippocampal slices are not attributable to deficient mitochondrial energy metabolism. *J Neurosci* **30:** 15638–15642

Ruusuvuori E, Li H, Huttu K, Palva JM, Smirnov S, Rivera C, Kaila K, Voipio J (2004) Carbonic anhydrase isoform VII acts as a molecular switch in the development of synchronous gamma-frequency firing of hippocampal CA1 pyramidal cells. *J Neurosci* **24:** 2699–2707

Schuchmann S, Hauck S, Henning S, Gruters-Kieslich A, Vanhatalo S, Schmitz D, Kaila K (2011) Respiratory alkalosis in children with febrile seizures. *Epilepsia* **52:** 1949–1955

Schuchmann S, Schmitz D, Rivera C, Vanhatalo S, Salmen B, Mackie K, Sipilä ST, Voipio J, Kaila K (2006) Experimental febrile seizures are precipitated by a hyperthermia-induced respiratory alkalosis. *Nat Med* **12:** 817–823

Schuchmann S, Vanhatalo S, Kaila K (2009) Neurobiological and physiological mechanisms of fever-related epileptiform syndromes. *Brain Dev* **31:** 378–382

Sinning A, Liebmann L, Kougioumtzes A, Westermann M, Bruehl C, Hubner CA (2011) Synaptic glutamate release is modulated by the Na^+-driven Cl^-/HCO_3^- exchanger Slc4a8. *J Neurosci* **31:** 7300–7311

Spray DC, Harris AL, Bennet MVL (1981) Gap junctional conductance is a simple and sensitive function of intracellular pH. *Science* **211:** 712–715

Stafstrom CE (2002) The incidence and prevalence of febrile seizures. In: *Febrile seizures*, Baram TZ, Shinnar S (eds). pp 1–25. Academic Press, San Diego

Staley KJ, Soldo BL, Proctor WR (1995) Ionic mechanisms of neuronal excitation by inhibitory GABA(A) receptors. *Science* **269:** 977–981

Sterling D, Reithmeier RAF, Casey JR (2001) A transport metabolon. Functional interaction of carbonic anhydrase II and chloride/bicarbonate exchangers. *J Biol Chem* **276:** 47886–47894

Stridh MH, Alt MD, Wittmann S, Heidtmann H, Aggarwal M, Riederer B, Seidler U, Wennemuth G, McKenna R, Deitmer JW, Becker HM (2012) Lactate flux in astrocytes is enhanced by a non-catalytic action of carbonic anhydrase II. *J Physiol* **590:** 2333–2351

Supuran CT (2008) Carbonic anhydrases: novel therapeutic applications for inhibitors and activators. *Nat Rev Drug Discov* **7:** 168–181

Swann JW, Smith KL, Brady RJ (1993) Localized excitatory synaptic-interactions mediate the sustained depolarization of electrographic seizures in developing hippocampus. *J Neurosci* **13:** 4680–4689

Tasker RC (1998) Emergency treatment of acute seizures and status epilepticus. *Arch Dis Child* **79:** 78–83

Thiry A, Dogne J, Supuran CT, Masereel B (2007) Carbonic anhydrase inhibitors as anticonvulsant agents. *Curr Top Med Chem* **7:** 855–864

Tolner EA, Hochman DW, Hassinen P, Otahal J, Gaily E, Haglund MM, Kubova H, Schuchmann S, Vanhatalo S, Kaila K (2011) Five percent CO_2 is a potent, fast-acting inhalation anticonvulsant. *Epilepsia* **52:** 104–114

Traynelis SF, Wollmuth LP, McBain CJ, Menniti FS, Vance KM, Ogden KK, Hansen KB, Yuan H, Myers SJ, Dingledine R (2010) Glutamate receptor ion channels: structure, regulation, and function. *Pharmacol Rev* **62:** 405–496

Truppo E, Supuran CT, Sandomenico A, Vullo D, Innocenti A, Di FA, Alterio V, De SG, Monti SM (2012) Carbonic anhydrase VII is S-glutathionylated without loss of catalytic activity and affinity for sulfonamide inhibitors. *Bioorg Med Chem Lett* **22:** 1560–1564

van Gassen KL, Hessel EV, Ramakers GM, Notenboom RG, Wolterink-Donselaar IG, Brakkee JH, Godschalk TC, Qiao X, Spruijt BM, van NO, De Graan PN (2008) Characterization of febrile seizures and febrile seizure susceptibility in mouse inbred strains. *Genes Brain Behav* **7:** 578–586

Velisek L, Dreier JP, Stanton PK, Heinemann U, Moshe SL (1994) Lowering of extracellular pH suppresses low-Mg^{2+} induced seizures in combined entorhinal cortex-hippocampal slices. *Exp Brain Res* **101:** 44–52

Viitanen T, Ruusuvuori E, Kaila K, Voipio J (2010) The KCl - cotransporter KCC2 promotes GABAergic excitation in the mature rat hippocampus. *J Physiol* **588:** 1527–1540

Voipio J, Kaila K (1993) Interstitial PCO^2 and pH in rat hippocampal slices measured by means of a novel fast CO_2/H^+-sensitive microelectrode based on a PVC-gelled membrane. *Pflugers Arch* **423:** 193–201

Voipio J, Pasternack M, Rydqvist B, Kaila K (1991) Effect of gamma-aminobutyric acid on intracellular pH in the crayfish stretch-receptor neurone. *J Exp Biol* **156:** 349–360

Waldmann R, Champigny G, Bassilana F, Heurteaux C, Lazdunski M (1997) A proton-gated cation channel involved in acid-sensing. *Nature* **386:** 173–177

Wang WG, Bradley SR, Richerson GB (2002) Quantification of the response of rat medullary raphe neurones to independent changes in pH_O and P_{CO_2}. *J Physiol* **540:** 951–970

Wilkins ME, Hosie AM, Smart TG (2005) Proton modulation of recombinant GABA(A) receptors: influence of GABA concentration and the beta subunit TM2-TM3 domain. *J Physiol* **567:** 365–377

Williams RH, Jensen LT, Verkhratsky A, Fugger L, Burdakov D (2007) Control of hypothalamic orexin neurons by acid and CO2. *Proc Natl Acad Sci USA* **104:** 10685–10690

Wimmer VC, Reid CA, Mitchell S, Richards KL, Scaf BB, Leaw BT, Hill EL, Royeck M, Horstmann MT, Cromer BA, Davies PJ, Xu R, Lerche H, Berkovic SF, Beck H, Petrou S (2010) Axon initial segment dysfunction in a mouse model of genetic epilepsy with febrile seizures plus. *J Clin Invest* **120:** 2661–2671

Supplemental information

Materials and methods

Generation of the CA VII KO mice. A clone isolated from a 129/SvJ mouse genomic λ library (Stratagene) was used to construct the targeting vector. A 12 kb fragment including exons 2 to 7 of the *Car7* gene was cloned into the pKO-V901 plasmid (Lexicon Genetics) with a phosphoglycerate kinase (pgk) promoter-driven diphtheria toxin A cassette. A pgk promoter-driven neomycin resistance cassette flanked by loxP-sites was inserted into the *Xho*I-site of intron 4. A third loxP-site and an additional *Eco*RI-site were inserted into the *Sac*II-site at the 3' end of the *Car7* gene. The construct was electroporated into R1 mouse embryonic stem cells. Neomycin resistant clones were analyzed by Southern blot using *Eco*RI and an external ~ 500 bp probe. Correctly targeted ES-cells were transfected with a plasmid expressing Cre-recombinase to remove the neomycin-cassette and exons 5, 6, and 7. Correctly recombined clones were identified with an internal probe by Southern blot analysis. Two independent embryonic stem cell clones were injected into C57BL/6 blastocysts to generate chimeras that were backcrossed with C57BL/6. Genotypes were either determined by Southern blot or by PCR on tail biopsy DNA. For PCR genotyping, the sense primer F1 (TGGAACGCCAAGAAGTACAGC) and the antisense primers R1 (ATGCCCTCACTGGGGAGATGG) and R2 (AGTCTTTATGGCAGAGACAGC) were used. The primer pair F1/R1 amplified a ~400 bp fragment of the wild-type allele, and the primer pair F1/R2 amplified a ~300 bp fragment of the knock-out allele. Mice were maintained on a 12 hour artificial light/dark cycle and provided with food and water *ad libitum*.

Matings between homozygous CA VII KO mice produced normal sized litters with viable pups. Hence, homozygous KO mating was used in addition to the heterozygous mating.

Generation of CA II/VII double KO mice. The heterozygous CA II and CA VII mice were used to generate mice devoid of both CA II and CA VII. The CA II/VII double KO animals were viable and born in the expected Mendelian ratio from heterozygous (~6.25 %, 9 out of the 194 genotyped animals) and homozygous CA VII/heterozygous CA II pairs (~12.5 %, 8 out of the 73 genotyped animals). The body weight of the CA II/VII KO's was smaller than that of their WT or heterozygous siblings as described previously for the CA II KO mice (Lewis et al.,

1988). For PCR genotyping of the CA II allele, primers WT-f (GTGAGTTACAGAGACAGAAG), WT-r (GGACTTTCTGAAGGACTTG), KO-f (GATTGGACCTGCCTCAT), and KO-r (GTTCTCTGGTTCTTGCATATG) were used to amplify fragments 237 bp (WT) and 163 bp (KO) in length.

Western analysis of muscle and liver tissue. For Western blotting, 10 µg protein lysates from hippocampus, skeletal muscle and liver were separated on reducing 15 % SDS-polyacrylamide gels and blotted onto a nitrocellulose membrane. Blots were probed with our rabbit CA VII antibody at a dilution of 1:250. Detection was done with Lasuser 3000 (Fujifilm) using chemoluminescence ECL-Kit (Pierce).

Solutions and slice preparation for pH_i and electrophysiological recordings. Transgenic mice (P5-46) or Wistar rats (P14) were decapitated, and the brains were dissected in ice cold (0-4 °C) solution. Coronal brain slices (350 µm) were cut with a vibrating blade microtome (Leica VT1000S). Dissection and preparation of the brain slices was done in modified standard solution containing (in mM) 87 NaCl, 70 sucrose, 2.5 KCl, 0.5 $CaCl_2$, 25 $NaHCO_3$, 1.1 NaH_2PO_4, 7 $MgSO_4$, and 25 D-glucose, equilibrated with 95% O_2, 5% CO_2. Slices were let to recover at 34°C for 30 minutes and then stored at room temperature. All recordings were performed in a submerged recording chamber at 32 ± 1°C, with one-sided perfusion, solution flow 4 ml/min. The standard solution contained (in mM) 124 NaCl, 3 KCl, 2 $CaCl_2$, 25 $NaHCO_3$, 1.1 NaH_2PO_4, 2 $MgSO_4$ and 10 D-glucose, equilibrated with 95% O_2, 5% CO_2, pH 7.4 at 32°C. In bicarbonate free, HEPES-buffered solution 25 mM $NaHCO_3$ was replaced with 10 mM NaOH, 10 mM NaCl and 20 mM HEPES (pH 7.4 at 32°C), and the solution was oxygenated with 100% O_2.

Detection of intrapyramidal carbonic anhydrase activity. In order to detect cytosolic CA activity, we exposed slices to nominally CO_2/HCO_3^- free HEPES solution for 100-200 s in the absence and presence of the membrane-permeant CA inhibitor acetazolamide (AZ 100 µM, Sigma-Aldrich, St.Louis, MO) and quantified the AZ induced suppression of the maximum rate of intracellular alkalinization (dpH_i/dt_{max}). Since AZ is known to inhibit both extra- and intracellular CA activity (Chesler, 2003), the control responses were done in the presence of the poorly permeant CA inhibitor benzolamide (BA, 10 µM) applied for 5 minutes before

withdrawal of CO_2/HCO_3^- to exclude effects mediated by inhibition of extracellular CAs. BA was a kind gift from Dr. E.R. Swenson (University of Washington, Seattle, WA).

pH_i was measured using the H^+-sensitive indicator BCECF. For the dye loading, brain slices were transferred to the recording chamber and perfused with standard solution. BCECF-AM (Invitrogen) was pressure-injected into the extracellular space of CA1 pyramidal layer using a conventional patch pipette, filled with 10 μM BCECF-AM in standard solution. In each slice, somatic pH_i was measured from 3-5 CA1 pyramidal neurons (see *Inset* in Figure 2*A*). Both loading and pH_i measurements were done in the continuous presence of TTX (1 μM).

Live-cell imaging was performed with an upright Zeiss Axio Scope II (60x water immersion objective n.a. 0.9). BCECF was excited with an OptoLED double wavelength light source (436 ± 10 nm and 500 ± 10 nm, Cairn, UK). Emitted light passed through a 535 ± 12.5 nm band pass filter and was registered with a PCO SensiCam CCD camera. The diameter of the region of interest (ROI) was about 3x5 μm, and the ROI was positioned at the site of the highest local signal. Ratiometric images were captured (at 0.1-0.2 Hz) and analyzed with WinFluor software (courtesy of Dr. John Dempster, University of Strathclyde, Glasgow, UK). For analysis the original pH-trace was smoothed with the Savitzky-Golay algorithm (20 data points frame, 2nd order polynomial) (Savitzky and Golay, 1964) and then differentiated with Origin software (OriginLab Corporation, Northampton, MA) using the equation:

$$\left(\frac{dpH_i}{dt}\right)_j = \frac{(pH_i)_{j+1} - (pH_i)_{j-1}}{t_{j+1} - t_{j-1}}$$

where *j* indicates the number of sample.

Electrophysiological recordings. Whole-cell patch-clamp recordings were performed from visually identified CA1 pyramidal cells. The glass micropipettes had a resistance of 4.5-6.0 MΩ when filled with intracellular solution consisting of (in mM) 124 K-gluconate, 5 KCl, 2 NaOH, 10 HEPES, 0.5 $CaCl_2$, 5 EGTA, 2 MgATP (pH adjusted to 7.3 with KOH). Recordings were made using an EPC 10 amplifier (HEKA Elektronik, Lambrecht/Pfalz, Germany) in the voltage-clamp or current-clamp mode and corrected for a calculated 15.0 mV liquid junction potential for whole-cell recordings (Barry, 1994). For field recordings, 4.5-6.0 MΩ glass microelectrodes were filled with the standard solution and placed in the stratum

pyramidale. The signal was high-pass filtered at 10 Hz. $GABA_A$ receptor-mediated synaptic responses were evoked in CA1 pyramidal neurons using a monopolar glass microelectrode filled with standard solution (resistance 4.5-6.0 MΩ, see Fig. 3) or, for a more intense $GABA_A$R activation, with a bipolar metal electrode, placed in the border of *stratum radiatum (sr) and* stratum lacunosum-moleculare *(slm)* (Alger and Nicoll, 1982;Staley et al., 1995;Kaila et al., 1997). The intensity of high-frequency stimulation (HFS; 40 pulses at 100 Hz, given every 5 minutes) applied via the bipolar electrode (Kaila et al., 1997) was sufficient to evoke near-maximal (≥ 80 %) $GABA_A$R responses, whereas the intensity of the monopolar stimulation (either single pulse stimulation at 15 s interval, or HFS) was adjusted to be slightly above the threshold of triggering $GABA_A$R-mediated responses with a negligible failure rate. $GABA_A$R-mediated responses were pharmacologically isolated by blocking ionotropic glutamate receptors with AP5 (40 µM) and CNQX (20 µM), and $GABA_B$ receptors with CGP-55845 (1 µM). $GABA_A$ receptors were blocked with PiTX (90 µM) or SR 95531 (50 µM), and DZP (1 µM) was used to enhance GABAergic transmission. Pressure microinjections of GABA (5 mM in standard solution) were applied via a glass capillary microelectrode (tip diameter 2–4 µm). Using Dodt gradient contrast, the apical dendrites of the CA1 pyramidal neurons were followed from site of recording to the border of *sr/slm*. The pressure injection pipette was placed to the border of *sr/slm* in the superficial layer of the slice. Brief pulses of pressure (18 pounds per square inch (psi), duration 8-100 ms) were given every 5 minutes. In these experiments TTX (1 µM) was used to prevent spiking, and CGP-55845 (1 µM) to block $GABA_B$ receptors. The drugs were from Tocris (Bristol, UK) except for diazepam which was a kind gift from Dr. Ari-Pekka Koivisto (Orion Pharma, Finland).

EEG measurements and FS induction.

Surgery and EEG recordings. On the day of experiments, typically two P13-14 animals from the same litter were studied. At this age CA VII KO mice were of comparable weight as their WT littermates (6.9 ± 0.2 g n = 11 vs. 6.4 ± 0.2 g, n = 9, respectively, P = 0.14, Student's t-test). For cortical EEG recordings ball-tipped Teflon-insulated silver wire electrodes (75 µm wire diameter, ball tip diameter ca. 1 mm; Advent Research Materials Ltd, Oxford, UK) were connected to microconnectors (Microtech Inc., Boothwyn, PA, USA) and fixed with dental acrylic. Electrodes were implanted under isoflurane anesthesia (maintained at 2-2.5 %).

Small craniotomies were made using a drill equipped with a 0.6 mm diameter carbide burr and electrodes were placed epidurally above right parietal cortex (AP 2.5 mm; ML 1.3 mm). A reference electrode was placed above cerebellum. The incision was sutured using 6-0 nylon monofilament. After surgery, mice recovered for two hours in a warm environment (35 °C) before the start of the experiment.

Before and during the induction of eFS, continuous cortical EEG and video recordings (Philips SPC 900 NC web camera; 25 frames/sec) were made from the freely moving mice. EEG signals were high-pass filtered (cut-off at 0.07 Hz) before 1000x amplification by a custom-made amplifier, and were sampled at 1 kHz using a 16-bit data acquisition interface and Labview software (National Instruments, Austin, Tx; custom-built functions courtesy of T. Maila).

Seizure induction. Seizures were induced using a heated chamber as described previously for neonatal rats (Schuchmann et al., 2006;2008). In parallel with the EEG and video recordings we monitored rectal temperature with a mouse rectal probe (BAT-10; Physitemp, Science Products GmbH, Hofheim, Germany) and breath rate with a piezo crystal sensor placed on the abdomen (Pico Movement Sensor; Temec, Kerkrade, Netherlands) (Schuchmann et al., 2008). After baseline recording at 30-34 ^{o}C for 10 minutes, pups were moved to a pre-heated chamber kept at 43 ± 1 ^{o}C for mice and at 48 ± 1 ^{o}C when rat pups were used. Animals were exposed to hyperthermia until their body temperature reached a critical high value of 42.5-43 ^{o}C (Dubé and Baram, 2006), after which the experiment was terminated and animals decapitated.

To test the effect of CO_2 on seizure generation, the heated chamber was supplied with a constant flow of pre-heated (43-44 °C) gas mixture of 5% CO_2, 19% O_2, and 76% N_2.

In experiments where diazepam was used (Stesolid Novum [Actavis], 5 mg/ml, diluted in 0.9% NaCl, injection volume 100 µl) the drug was given intraperitoneally (i.p.) at 50 µg/kg, 150 µg /kg or 2.5 mg/kg dose 15 minutes before the onset of hyperthermia. An equal volume of saline was injected into control animals.

Data analysis. EEG, breathing, temperature and video-recordings were analyzed off-line using Diadem 10.0 software (National Instruments, Austin, Tx). Electrographical seizure activity was recognized as bursts of regular spikes with amplitude values around 150-600 µV which is at least 3x standard deviation of baseline EEG amplitude with durations of 10

seconds up to 1 minute. Breath rate (breaths/min) was analyzed in the baseline period and hyperthermia. During hyperthermia, for WT animals the breath rate was analyzed within the minute just before EEG seizure onset, on average around the 24th minute (see Results). For CA VII KO mice, the breathing rate during hyperthermia was analyzed around the 24th minute after the start of hyperthermia. Detection of movement artefacts in the EEG traces was done using the piezo-transducer signal (see above) and the video.

Blood samples. To measure hyperthermia induced change in blood pH and electrolytes, we collected blood samples from control WT and CA VII KO mice and from WT and CA VII KO mice that were exposed to hyperthermia. From each animal 80 µl of blood was collected after decapitation into plastic capillaries (1.9x54 mm) with lyophilised lithium-heparin 100 I.U./ml (Sanguis Counting GmbH, Numbrecht, Germany) and pH was measured with GEM Premier 4000 device (Instrumentation Laboratory, USA).

From control animals the sample was collected after breathing rate and rectal temperature were recorded for 10 minutes. Animals that underwent hyperthermia were placed in a pre-heated chamber (43 ± 1 ^{o}C) after baseline measurement of breathing rate and body temperature. The blood sample was collected after the body temperature reached 41.5 ^{o}C. In experiments with EEG recordings all WT mice had developed seizures at this point.

Detection of CA VII in the developing human neorcortex and hippocampus.

Exon array analysis was performed as previously described (Kang et al., 2011). Briefly, total RNA was isolated from specific brain regions of neocortex and hippocampus using a non-phenolic procedure (RNeasy Plus Mini Kit, Qiagen), followed by DNase treatment (TURBO DNase, Ambion). Optical density values at 260/280 were consistently above 1.9 (NanoDrop, Thermo Scientific), and the values of RNA integrity were selected above 5 (RIN>5, Agilent Bioanalyzer). Synthesized cDNA (5.5 µg) using WT Expression kit (Ambion) was labeled and loaded onto individual Affymetrix Human Exon 1.0 ST arrays. Microarrays were hybridized at 45 °C for 16–24 hours, washed and stained using an Affymetrix FS450 fluidics station, according to manufacturer recommendations. Microarrays were scanned on a GeneChip Scanner 3000 and visually inspected for hybridization artifacts. The raw image files (.DAT files) were analysed using Affymetrix GeneChip Operating Software to generate .CEL files.

Droplet digital PCR. An aliquot of the total RNA that was previously extracted from each brain region was used for secondary validation using droplet digital PCR analysis.

One ug of total RNA was used for cDNA synthesis using oligo dT primers and SuperScript III First-strand synthesis Supermix (Invitrogen), and subsequently diluted with nuclease-free water to 1 ng/ul cDNA. Gene-specific high-melt temperature primers and FAM-probes for genes of interest were designed using PrimerQuest℠ (http://www.idtdna.com/Scitools/Applications/Primerquest) and expressed sequence information obtained from GenBank (NCBI). PCR reactions were conducted on the QX100 Droplet Digital™ PCR system (Bio-Rad) according to manufacturer recommendations. Briefly, the reaction mixture containing sample cDNA, primers and probe was partitioned into about 20,000 droplets in oil through the QX100 Droplet Generator. After PCR amplification (95'C 10 min; 40 cycles of (94'C 30 sec, 57'C 60 sec); 98'C 2 min), each droplet provided a positive or negative fluorescent signal indicating the target gene was present or not present after partitioning. Positive and negative droplets were counted in the QX100 Droplet Reader and the software calculated the concentration of target gene as copies per microliter. The copy number of *CA VII* was normalized to the housekeeping gene *Gapdh*.

References

Alger BE, Nicoll RA (1982) Pharmacological evidence for two kinds of GABA receptor on rat hippocampal pyramidal cells studied in vitro. J Physiol 328:125-141.

Barry PH (1994) JPCalc, a software package for calculating liquid junction potential corrections in patch-clamp, intracellular, epithelial and bilayer measurements and for correcting junction potential measurements. J Neurosci Methods 51:107-116.

Chesler M (2003) Regulation and modulation of pH in the brain. Physiol Rev 83:1183-1221.

Dubé CM, Baram TZ (2006) Complex febrile seizures - An experimental model in immature rodents. In: Models of seizures and epilepsy (Pitkanen A, Schwartzkroin PA, Moshe SL, eds), pp 333-340. Elsevier Academic Press.

Kaila K, Lamsa K, Smirnov S, Taira T, Voipio J (1997) Long-lasting GABA-mediated depolarization evoked by high- frequency stimulation in pyramidal neurons of rat hippocampal slice is attributable to a network-driven, bicarbonate-dependent K+ transient. J Neurosci 17:7662-7672.

Kang HJ, et al. (2011) Spatio-temporal transcriptome of the human brain. Nature 478:483-489.

Lewis SE, Erickson RP, Barnett LB, Venta PJ, Tashian RE (1988) N-ethyl-N-nitrosurea induced mutation at the mouse Car-2 locus - an animal model for human carbonic anhudrase II-deficiency syndrome. Proc Natl Acad Sci U S A 85:1962-1966.

Savitzky A, Golay MJE (1964) Smoothing and differentation of data by simplified least squares procedures. Anal Chem 36:1627-1639.

Schuchmann S, Schmitz D, Rivera C, Vanhatalo S, Salmen B, Mackie K, Sipila ST, Voipio J, Kaila K (2006) Experimental febrile seizures are precipitated by a hyperthermia-induced respiratory alkalosis. Nat Med 12:817-823.

Schuchmann S, Tolner EA, Marshall P, Vanhatalo S, Kaila K (2008) Pronounced increase in breathing rate in the "hair dryer model" of experimental febrile seizures. Epilepsia 49:926-928.

Staley KJ, Soldo BL, Proctor WR (1995) Ionic mechanisms of neuronal excitation by inhibitory GABA(A) receptors. Science 269:977-981.

Figure S1 Ruusuvuori et *al.*

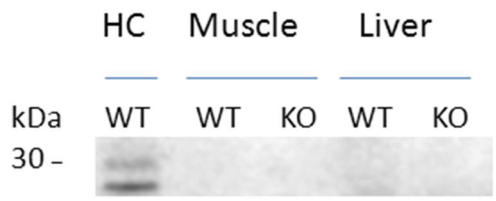

Supplemental Figure S1

CA VII protein is not present in skeletal muscle or liver. In agreement with the Northern analysis shown in Fig. 1B, Western analysis of adult WT mouse muscle and liver does not show any CA VII protein expression while a robust signal is seen in WT hippocampal tissue (HC) (see also Fig. 1C).

Figure S2 Ruusuvuori et *al.*

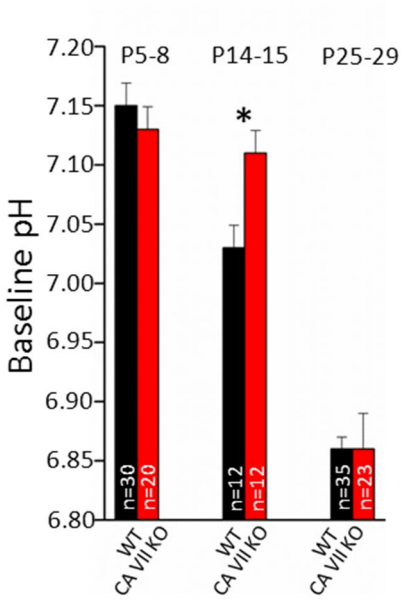

Supplemental Figure S2

Expression of cytosolic carbonic anhydrase changes somatic pH in CA1 pyramidal neurons. Intraneuronal pH measurements were performed with BCECF in slice preparations from P5-29 WT and CA VII KO mice. At P5-8 the baseline pH_i was similar in neurons from WT and CA VII KOs (mean + SEM; $P = 0.5$). In WT mice expression of CA VII starts at around P10 and causes an intraneuronal acidification (P14-15). In CA VII KO neurons pH_i remained at significantly more alkaline level ($P = 0.011$). This pH-difference is not seen in more mature neurons (P25-29) after the onset of CA II expression ($P = 0.78$). Numbers in bar diagrams denote the number of cells. *P*-values are based on Student's *t*-test (*$P < 0.05$).

Figure S3 Ruusuvuori et *al.*

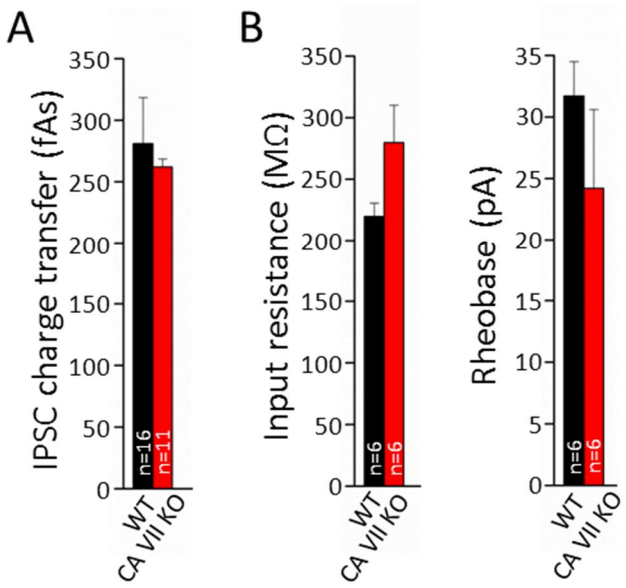

Supplemental Figure S3

The single inhibitory postsynaptic currents and the intrinsic excitability of CA1 pyramidal neurons are similar in WT and CA VII KO at P12-16. (A) The apparent charge transfer associated with single inhibitory postsynaptic currents (IPSCs) did not differ between the two genotypes (mean + SEM; *P* = 0.75). Measurements were made under voltage clamp conditions (V_m -70 mV) with minimal stimulation delivered to distal dendrites at 0.25 Hz. (B) The input resistance (R_{in}; *P* = 0.09) and the rheobase (*P* = 0.31) were comparable in the WT and CA VII KOs neurons. Numbers in bar diagrams denote the number of cells and *P*-values are based on Student's *t*-test.

Figure S4 Ruusuvuori et *al.*

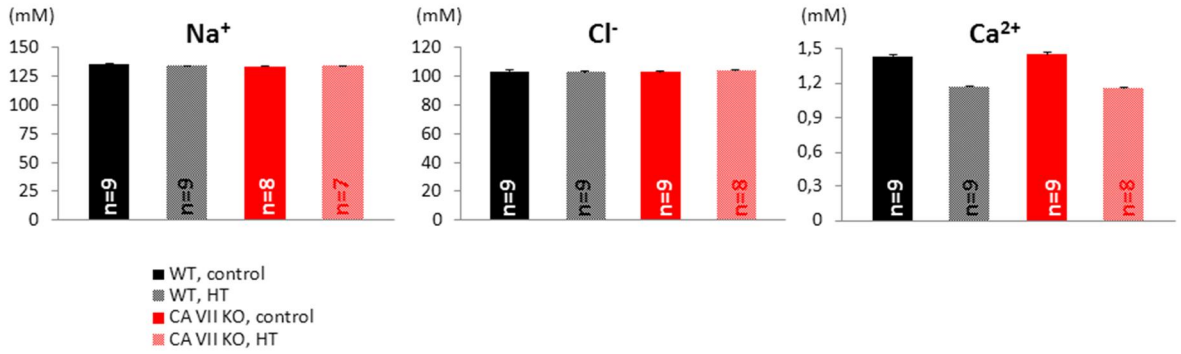

Supplemental Figure S4

Blood electrolyte values do not show genotype-specific differences in control or under hyperthermia. Under control conditions blood electrolyte levels in WT and CA VII KO mice had almost identical mean values and overlapping SEM values (Na^+: 135±0.8 mM vs. 134±0.4 mM; Cl^-: 103±0.8 mM vs. 103±0.4 mM; Ca^{2+}: 1.43±0.02 mM vs. 1.45±0.02 mM, respectively). Calcium, but not sodium and chloride, underwent a quantitatively identical decrease in hyperthermia (HT) in WT and CA VII KO mice (Ca^{2+} under hyperthermia 1.17±0.01 mM and 1.15±0.01, respectively). Values are given as mean + SEM, the number of animals is indicated in the bar diagram.

Figure S5 Ruusuvuori et *al.*

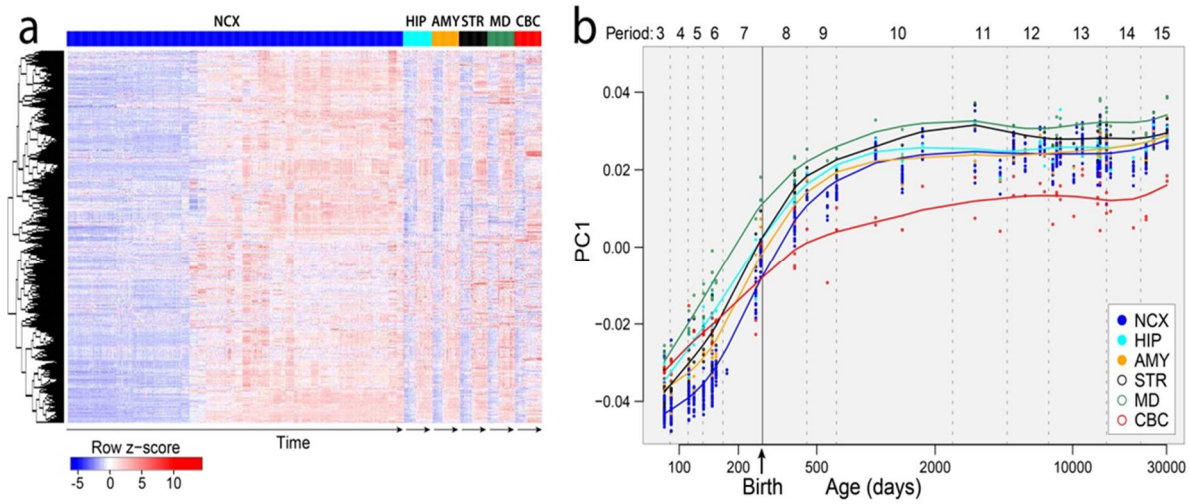

Supplemental Figure S5

WGCNA Module 2. M2 was associated with a progressive increase in gene expression across all regions starting at the embryonic period. (A) Heat map of genes in M2 after hierarchical clustering showing the temporally co-expressed pattern is consistent across all regions. The expression values for each gene were ordered first by brain regions, then by age, and last by neocortex areas. (B) The spatio-temporal pattern of M2 was summarized using PCA analysis. PC1 was plotted against age, after being grouped and color-coded according to brain regions. Neocortex (NCX), hippocampus (HIP), amygdala (AMY), striatum (STR), mediodorsal nucleus of the thalamus (MD), and cerebellar cortex (CBC). The pattern was summarized by the smoothed curves of PC1 values. Dashed lines represent division between periods of the development, and the solid line separates prenatal from postnatal periods